合成孔径雷达三维成像——从层析、阵列到微波视觉(中文/English)

丁赤飚*①②④ 仇晓兰*①③④ 徐 丰⑤ 梁兴东①②④ 焦泽坤①② 张福博①②④

①(中国科学院空天信息创新研究院 北京 100190)
②(微波成像技术国家级重点实验室 北京 100190)
③(中国科学院空间信息与应用系统重点实验室 北京 100190)
④(中国科学院大学 北京 100049)
⑤(复旦大学 上海 200433)

摘 要：合成孔径雷达3维成像技术可以消除目标和地形在2维图像上产生的严重混叠，显著提升目标识别和3维建模能力，已经成为当前SAR发展的重要趋势。合成孔径雷达3维成像技术经过了数十年的发展，已提出多种技术体制。该文系统性回顾了SAR 3维成像技术领域的发展过程，深入分析了现有SAR 3维成像技术的特点；指出了SAR回波及图像中蕴含的未被现有技术利用的3维信息，提出“合成孔径雷达微波视觉3维成像”的新概念和新思路，将SAR成像方法与微波散射机制和图像视觉语义有机融合，形成SAR微波视觉3维成像理论与方法，实现高效能、低成本的SAR 3维成像。该文重点阐述了SAR微波视觉3维成像的概念、目标和关键科学问题，并给出了初步的技术途径，为SAR 3维成像提供了新的技术思路。

关键词：合成孔径雷达3维成像；阵列干涉；层析SAR；SAR微波视觉3维成像

中图分类号：TN957.52 **文献标识码**：A **文章编号**：2095-283X(2019)06-0693-17

DOI: 10.12000/JR19090

引用格式：丁赤飚, 仇晓兰, 徐丰, 等. 合成孔径雷达三维成像——从层析、阵列到微波视觉[J]. 雷达学报, 2019, 8(6): 693–709. doi: 10.12000/JR19090.

Reference format: DING Chibiao, QIU Xiaolan, XU Feng, *et al*. Synthetic aperture radar three-dimensional imaging ——from TomoSAR and array InSAR to microwave vision[J]. *Journal of Radars*, 2019, 8(6): 693–709. doi: 10.12000/JR19090.

Synthetic Aperture Radar Three-dimensional Imaging——From TomoSAR and Array InSAR to Microwave Vision (in English)

DING Chibiao*①②④ QIU Xiaolan*①③④ XU Feng⑤ LIANG Xingdong①②④
JIAO Zekun①② ZHANG Fubo①②④

①(*Aerospace Information Research Institute, Chinese Academy of Sciences, Beijing* 100190, *China*)
②(*National Key Lab of Microwave Imaging Technology, Beijing* 100190, *China*)
③(*Key Laboratory of Technology in Geo-spatial Information Processing and Application System, Beijing* 100190, *China*)
④(*University of Chinese Academy of Sciences, Beijing* 100049, *China*)
⑤(*Fudan University, Shanghai* 200433, *China*)

Abstract: Synthetic Aperture Radar three-Dimensional (SAR 3D) imaging technology can eliminate severe overlap in 2D images, and improve target recognition and 3D modeling capabilities, which have become an

收稿日期：2019-09-30；改回日期：2019-11-04

*通信作者： 仇晓兰 xlqiu@mail.ie.ac.cn； 丁赤飚 cbding@mail.ie.ac.cn

*Corresponding Author: QIU Xiaolan, xlqiu@mail.ie.ac.cn; DING Chibiao, cbding@mail.ie.ac.cn

基金项目：国家自然科学基金重大项目“合成孔径雷达微波视觉三维成像理论与应用基础研究”(61991420, 61991421)

Foundation Items: The Major Program of National Natural Science Foundation of China “Research on SAR Microwave Vision Three-Dimensional Imaging Theory and Application Fundation”(61991420, 61991421)

责任主编：张群 Corresponding Editor: ZHANG Qun

important trend in SAR development. After decades of development of SAR 3D imaging technology, many types of 3D imaging methods have been proposed. In this study, the history of SAR 3D imaging technology is systematically reviewed and the characteristics of existing SAR 3D imaging technology are analyzed. Given that the 3D information contained in SAR echo and images is not fully used by existing techniques, a new concept of SAR microwave vision 3D imaging has been proposed for the first time. This new concept is integrated with microwave scattering mechanism and image visual semantics to realize three-dimensional reconstruction, which form the theory and method of SAR microwave vision 3D imaging and can achieve high-efficiency and low-cost SAR 3D imaging. This study also analyzes the concept, goal and key scientific problems of SAR microwave vision 3D imaging and provides a preliminary solution, which will contribute in several ways to our understanding of SAR 3D imaging and provide the basis for further research.

Key words: SAR 3D imaging; Array InSAR; SAR Tomography; SAR microwave vision 3D imaging

1 引言

以合成孔径雷达(Synthetic Aperture Radar, SAR)为代表的微波成像技术是高分辨率对地观测的重要技术手段，在军事侦查、地形测绘、环境监测、地质勘探和灾情调查等方面具有重大应用价值。然而，由于SAR与光学成像机理显著不同，SAR目标识别与图像解译难度极大，已成为制约当前星载和机载SAR装备应用效能有效发挥的关键瓶颈。其中的重要原因是传统SAR只能获取2维影像，在地形变化陡峭和环境复杂的区域，3维目标在2维图像上会产生严重混叠，导致大量目标看不清、辨不明、难以理解。SAR 3维成像可以直接获得目标的3维电磁散射结构，消除SAR图像中由于成像机理导致的收缩、叠掩、顶底倒置等现象，对3维环境构建、目标精细化解译、城市测绘以及灾害评估等应用具有重大意义。

在此背景下，SAR 3维成像技术受到了各国的重视，不断发展进步。以是否具备3维分辨能力为区分，SAR成像从2维到3维的发展过程大致可以划分为两个阶段。第1个阶段从上世纪60年代起，发展出干涉合成孔径雷达[1](Interferometric SAR, InSAR)和SAR立体像对技术[2,3](StereoSAR)，以获得场景3维信息。然而，InSAR和StereoSAR技术本质上均是利用不同角度观测对配准后的像素进行3维位置的解算，对于同一像素中叠掩多个散射点的情况，只能求解合成散射中心的位置，因此仅能够获得3维表面信息，不具备3维分辨能力。第2阶段则从上世纪九十年代起，1995年美国海军研究实验室的K. K. Knaell和G. P. Cardillo[4]首次提出了3维SAR的概念，并提出了利用高度维的合成孔径实现3维成像的技术思路。在此之后，美国、欧洲、中国等均开展了大量SAR 3维成像的研究工作[5–11]，目前主要形成了两种3维成像技术，分别是合成孔径雷达层析成像技术(SAR Tomography, TomoSAR)和阵列干涉SAR 3维成像技术(Array InSAR)。上述两种SAR 3维成像技术通过多次航过或多个天线的多角度观测，形成高度维的合成孔径，获得第3维分辨能力。然而上述技术需要大量的多角度观测，导致成像周期长或系统高度复杂，推广应用存在较大的难度。

综观SAR 3维成像技术发展，从早期的干涉SAR技术到现阶段的TomoSAR 3维成像技术，本质上讲均为利用精确的雷达成像几何物理模型，结合多角度观测进行目标3维位置解算。而实际上，在单幅SAR图像中，蕴含了场景与目标的结构、纹理、遮挡关系等3维空间线索，这些有效信息在目前的成像体制中尚未得到充分的挖掘与利用。本文提出了一种新的SAR 3维成像技术，称之为“合成孔径雷达微波视觉3维成像”技术，通过对微波散射机制和图像视觉语义的深入挖掘，提取雷达回波和2维图像中蕴含的3维线索，结合传统的SAR成像理论，实现高效3维成像，大幅减少所需观测的数目。

本文首先深入分析了当前合成孔径雷达3维成像技术的基本原理、技术特点和局限性。在此基础上，提出了合成孔径雷达微波视觉3维成像技术，详细介绍了SAR微波视觉3维成像技术的概念、内涵和关键科学问题，并给出了初步的技术途径，最后对未来的发展进行了展望。

2 TomoSAR 3维成像技术

2.1 TomoSAR 3维成像原理

针对大量存在叠掩现象的城区等复杂场景3维重建的目的，国内外研究机构开展了大量研究，借鉴医学CT(Computed Tomography)成像技术，提出了层析SAR(SAR Tomography, TomoSAR) 3维成像技术。层析SAR 3维成像原理如图1所示。

图1展示了TomoSAR技术3维分辨能力的来源。与传统2维SAR成像相同，距离向通过发射大带宽信号结合脉冲压缩技术获得距离分辨率，方位

向通过合成孔径获取分辨能力。为了获得高程向分辨能力，利用航迹精确控制、满足奈奎斯特定律的多次观测构建高程向的等效阵列，实现高度维的合成孔径，获得高程向分辨能力。TomoSAR 3维成像几何模型如图2所示[7]，利用较小视角差异的多幅SAR图像，经图像配准后，逐像素进行解算。

TomoSAR成像数学模型如下，第n次观测得到SAR图像像素表达式如式(1)[6]

$$y_n = \int_{\Delta s} \gamma(s) \exp\left[-\mathrm{j}\frac{4\pi}{\lambda} R_n(s)\right] \mathrm{d}s \tag{1}$$

针对同一像素，多次观测得到的像素值构成观测向量$\boldsymbol{y}$，将高程向离散化可以得到观测方程为

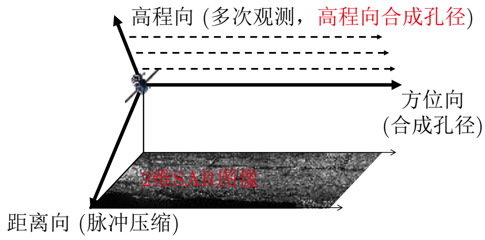

图 1 TomoSAR 3维成像原理图

Fig. 1 Diagrammatic sketch of TomoSAR 3D imaging

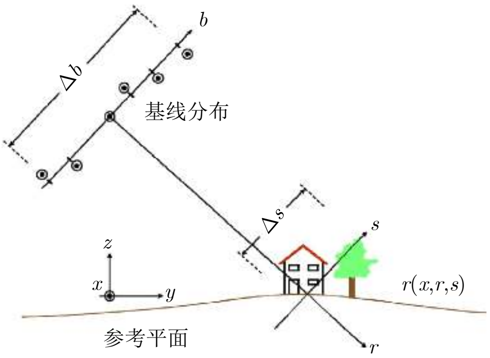

图 2 TomoSAR 3维成像几何原理图

Fig. 2 TomoSAR imaging geometry

$$\boldsymbol{y} = \boldsymbol{\Phi}\boldsymbol{\gamma} + \boldsymbol{n} \tag{2}$$

其中，$\boldsymbol{\Phi}_{i,j} = \exp(-\mathrm{j}4\pi/\lambda \cdot \Delta b_i s_j / R_0)$。根据式(2)即可求解得到目标散射系数沿高程向分布$\boldsymbol{\gamma}$。

2.2 TomoSAR 3维成像研究现状

层析SAR 3维成像技术研究始于上世纪九十年代中期，其技术发展经过了实验室研究、机载层析成像以及星载层析成像3个阶段。1995年，欧洲微波信号实验室(European Microwave Signature Laboratory, EMSL)的Pasquali等人[8]首次证明了利用多次观测在高程向合成孔径实现高度维分辨是可行的，该实验室设计了具有8条基线的Ku波段雷达系统，对隐藏在介质中的两层金属球实现了高度维分辨，实现了层析SAR 3维成像技术从理论到实验的跨越。1998年，德国宇航局(Deutsches Zentrum für Luft- und Raumfahrt, DLR)的Reigber等人[9]开展了机载层析SAR成像技术的研究，利用L波段的机载SAR实测数据实现了对建筑和植被3维结构的重建，是世界上首个机载层析SAR 3维成像结果。2005年，意大利那不勒斯大学的Fornaro等人[10]利用欧洲遥感卫星(European Remote Sensing Satellite, ERS)在1992年至1998年间获取的意大利Naples地区30景SAR图像，首次实现了星载层析SAR 3维成像。2007年，德国TerraSAR-X(TSX)卫星发射，该卫星具有良好的控轨能力和极高的相位测量精度，聚束模式SAR图像分辨率可达1 m，进一步促进了TomoSAR技术的发展。2010年，德宇航的朱晓香等人[12]利用TerraSAR-X数据，首次获得了复杂城市场景(如LasVegas)的层析3维成像结果，见图3。在此之后，该团队又利用该卫星数据开展了丰富的星载TomoSAR研究，在层析SAR 3维成像算法方面取得了丰富的成果[13–18]。

伴随着更多全极化星载与机载SAR系统的投入使用，极化层析SAR(Polarimetric TomoSAR,

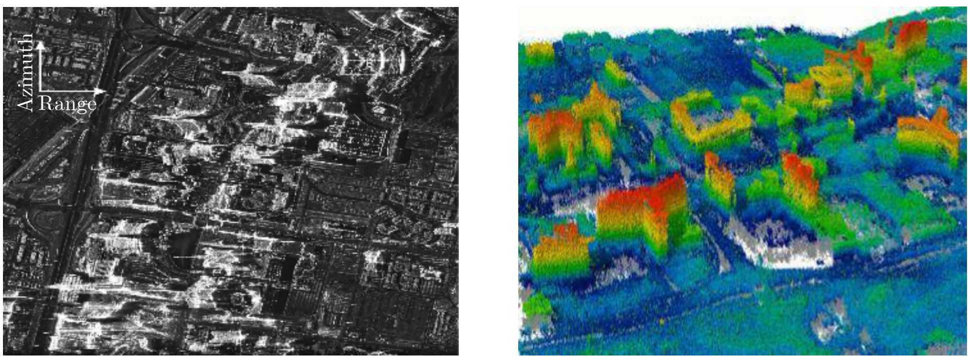

(a) 美国LasVegas地区SAR图像 (TerraSAR-X)
(a) TerraSAR-X radar image of LasVegas

(b) LasVegas地区TomoSAR 3维点云
(b) TomoSAR 3D point cloud of LasVegas

图 3 2010年，德宇航首个城区TomoSAR 3维成像[12]

Fig. 3 TomoSAR 3D imaging result of urban areas by DLR in 2010[12]

PolTomoSAR)技术应运而生，在森林生物量反演等应用中发挥重大作用[19]。此外，由于普通的TomoSAR成像从一个角度进行观测，SAR图像阴影区域无法实现层析成像，因此德国开展了机载圆迹层析(SAR Holography, HoloSAR)成像技术研究，实现了360度观测的3维成像[20]。图4展示了极化层析及HoloSAR 3维成像的部分结果。国内也纷纷开展TomoSAR技术的研究，中国科学院电子学研究所、武汉大学、电子科技大学等单位[21–24]均在TomoSAR成像算法方面取得了丰富的成果。

2.3 TomoSAR技术特点

TomoSAR 3维成像技术在城区等复杂地区3维成像中取得了巨大成功，然而在实际应用中面临两大主要困难。第一，利用传统信号处理方法(如匹配滤波、谱估计等)，需要数十次甚至上百次飞行，周期长、成本高，不利于时效性要求较高的应用。第二，为了保证TomoSAR重轨观测SAR图像之间的相干性，需要实现航迹的精确控制，增加了实施的难度。

由于层析SAR 3维成像理论针对每一个距离方位单元进行处理，地物目标在高程向稀疏分布，因此压缩感知理论的提出为第1个问题提供了解决思路。2006年由Donoho等人[25]提出的压缩感知(Compressed Sensing, CS)理论，突破了奈奎斯特定律的限制，在满足稀疏性假设的前提下，能够利用少数观测以较高概率重建原始信号。2007年，Baraniuk等人[26,27]提出将压缩感知理论应用到雷达成像中。2009年，意大利的Alessandra Budillion等人[28,29]基于压缩感知理论进行了层析SAR仿真实验，指出压缩感知理论可以减少目标3维重构所需重轨观测次数，之后又将该技术应用于ERS卫星数据，成功实现了建筑物的3维成像。同年，DLR的朱晓香团队[16]将压缩感知理论应用于TerraSAR-X的高分辨率数据，获取了TerraSAR实测数据层析成像结果。2011年，该团队提出了SLIMMER算法并系统分析了算法性能。近年来，国内外学者针对结合压缩感知理论的层析成像开展了大量研究，在稀疏成像算法等方面成果丰硕[17,18,30–32]。图5展示了观测稀疏化前后层析成像结果的对比，利用7景图像实现了TomoSAR 3维成像，相比64景图像重建结果分辨率差异较小，证实了航迹稀疏化的可行性。

为了保证TomoSAR重复观测图像之间相干性，需要层析SAR重轨观测基线较短，避免空间去相关，对于重复观测的轨道控制精度提出了较高要求。随着卫星控轨技术的进步，诸如TerraSAR-X等卫星控轨精度已较高，如TerraSAR-X多次重复观测，相对于参考航迹轨道控制精度优于500 m，所有重轨观测航迹控制在以参考航迹为轴心250 m为半径的“管道”内(如图6所示)，尤其在径向，重复轨道控制精度优于100 m[33]，轨道测量精度则优于10 cm。目前，如TerraSAR-X, Cosmo-Skymed等高分辨率星载SAR系统均具有较高的轨道控制与测量精度[33–37]，星载SAR的轨道控制精度已经能够满足TomoSAR的处理需求，但是机载系统由于受到气流等的影响，获得有效的TomoSAR数据非常困难。

总之，目前TomoSAR 3维成像处理仍然需要十余次严格控轨的重复观测，时间跨度较长，难以满足时效性要求较高的应用场景。

3 阵列干涉SAR 3维成像技术

3.1 下视阵列3维成像研究

下视阵列合成孔径雷达3维成像技术是一种基

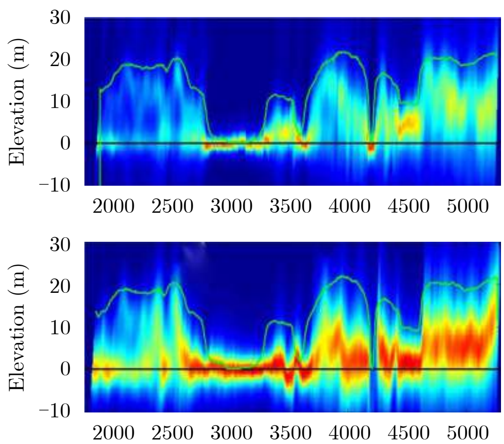

(a) 极化层析SAR 3维成像结果[19]
(a) PolTomoSAR 3D imaging results[19]

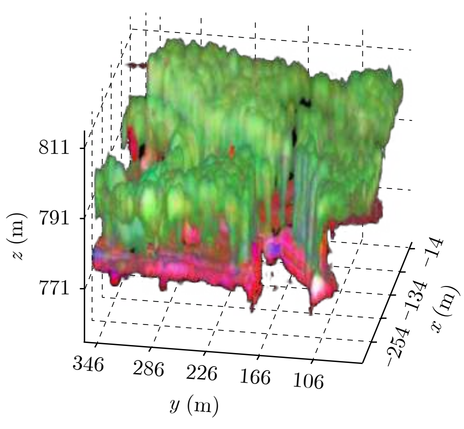

(b) HoloSAR森林3维成像结果[20]
(b) HoloSAR 3D imaging results of forest[20]

图 4 极化层析SAR与HoloSAR 3维成像
Fig. 4 Three-dimensional imaging results of PolTomoSAR and HoloSAR

(a) 联邦铁路公司总部光学图像
(a) Optical image

(b) 联邦铁路公司总部TerraSAR-X雷达图像
(b) TerraSAR-X radar image

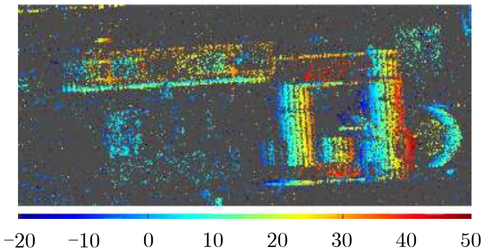

(c) 64景TerraSAR-X图像TomoSAR重建结果
(c) TomoSAR results with 64 images

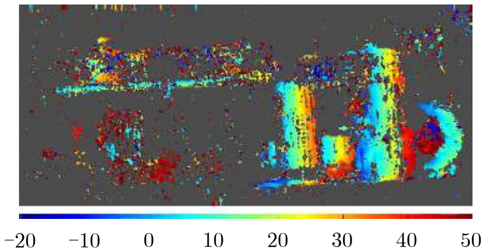

(d) 7景TerraSAR-X图像TomoSAR重建结果
(d) TomoSAR results with 7 images

图 5 德国联邦铁路公司总部层析成像结果[32]

Fig. 5 TomoSAR imaging results of DB Headquarters in Munich[32]

(a) 德国TerraSAR-X卫星
(a) TerraSAR-X satellite

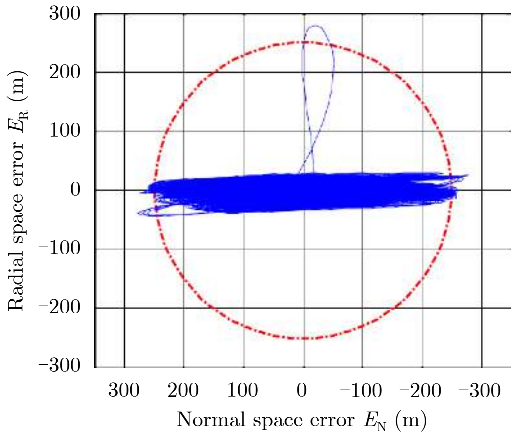

(b) 2009年第4季度TSX轨道控制情况
(b) TSX orbit control performance during 4th quarter of 2009

图 6 TerraSAR-X卫星轨道控制精度示意图[33]

Fig. 6 Diagrammatic sketch of TSX orbit control performance[33]

于阵列天线的SAR 3维成像技术，通过在跨航向安装阵列天线，以期对载机平台正下方场景实现3维成像。下视阵列3维成像技术工作示意图见图7。

下视阵列3维成像技术向飞机正下方发射宽带信号，结合脉冲压缩技术实现高程向分辨；在方位向借助平台运动获得航迹向多普勒信息，形成合成孔径，实现方位向分辨；在跨航向借助阵列天线实现跨航向合成孔径，进而实现跨航向分辨。

1999年，DLR首次提出了下视2维成像雷达的概念[38]。2004年，法国ONERA的Giret等人[39]提出了下视阵列3维成像技术，将阵列技术和合成孔径雷达相结合，能够获得跨航向、方位向和高程向的分辨能力。之后，其开始研制相应下视阵列3维成

图 7 下视阵列3维成像技术示意图

Fig. 7 Diagrammatic sketch of downward looking array 3D imaging

像系统DRIVE，该系统具有下视3维和正侧视2维两种工作模式，试验载机是翼展23 m重约900 kg的滑翔机[40]。2006年至2010年间，Nouvel等人[41]利用DRIVE系统开展了下视阵列成像试验，并公开了方位向长度1 km的方位-高程2维成像结果(见图8)，其中跨航向测绘带宽度为42 m。德国FGAN-FHR的Klare等人[42,43]从2005年开始研制无人机下视阵列3维SAR系统ARTINO，载机翼展4 m、重量25 kg。2010年，针对定标点开展了飞行试验，但没有公布3维成像结果[44]。国内中国科学院电子学研究所、电子科技大学等单位[45,46]针对下视阵列3维成像开展研究，在成像算法以及试验装置研究等方面取得了丰富成果。

然而，下视阵列SAR受限于成像体制，存在以下问题：首先，下视阵列SAR测绘带宽一般较窄，例如DRIVE系统跨航向测绘带宽仅42 m，工作效率低下；其次，由于阵列下视SAR在跨航向采用实孔径进行分辨，为解决分辨率和测绘带宽之间的矛盾，需要系统具有很多的通道数量，使得系统具有较高的复杂度，成本较高；最后，由于采用下视模式，且阵列天线长度受限，其跨航向分辨率较低，3维重建点云密度较低，3维成像性能较差。截至目前，国内外尚未见下视阵列3维SAR的3维场景成像结果公开发表。

3.2 阵列干涉SAR 3维成像系统

针对下视阵列SAR 3维成像技术存在的问题，中科院电子所提出了阵列干涉SAR(Array InSAR)技术进行3维成像。阵列干涉SAR进行侧视成像，利用跨航向的阵列天线，基于多输入多输出技术(Multi-Input Multi-Output, MIMO)虚拟多个天线等效相位中心，通过接收地物回波获取多通道相干SAR图像，一次飞行即可得到多角度观测数据，可以实现单次航过3维成像，相干性好、时效性强。相比下视阵列3维成像技术，阵列干涉SAR 3维成像采用侧视工作模式，测绘带更宽；等效相位中心数量远小于下视阵列系统，系统复杂度较低，具有更高的稳定性和易实现性；距离向分辨率更佳，重建点云密度高，3维成像性能相对优秀。阵列干涉SAR 3维成像原理如图9所示。

中科院电子所[47,48]2005年开始研制阵列干涉

(a) ARTINO 3维成像概念图[42]
(a) Diagrammatic sketch of ARTINO[42]

(b) ARTINO下视阵列系统实物图[43]
(b) MIMO antenna array of ARTINO[43]

(c) 法国DRIVE系统载机BUSARD滑翔机[40]
(c) ONERA BUSARD motorglider[40]

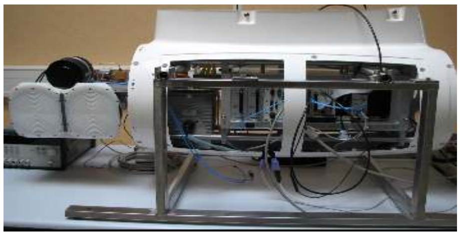

(d) DRIVE系统Ka波段雷达系统[40]
(d) Ka radar system of DRIVE[40]

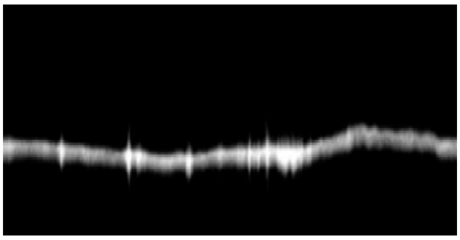

(e) DRIVE系统成像结果方位-高程平面2维切片[41]
(e) Imaging result of DRIVE in the azimuth-elevation plane[41]

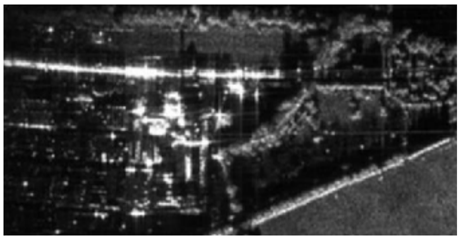

(f) 同一区域侧视2维SAR图像
(f) 2D SAR image of the same area

图 8 全球阵列SAR 3维成像系统

Fig. 8 Global array 3D imaging systems

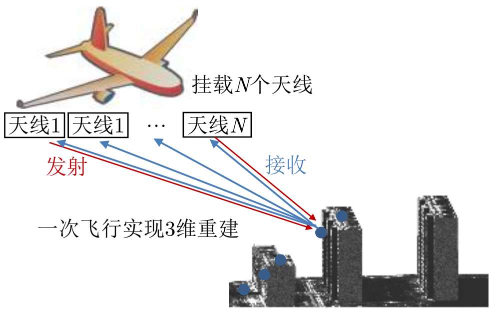

图 9 阵列干涉SAR 3维成像示意图

Fig. 9 Diagrammatic sketch of Array InSAR 3D imaging

SAR系统，采用长2 m重150 kg的刚性天线阵来保证基线的稳定性，通过毫米级的基线高精度定标、以及基于阵列图像匹配干涉和逐像素3维解算的3维成像处理方法，于2015年获得了国际首幅3维场景成像结果。该系统融合了多通道的分辨能力和相干测量的高精度两项优势，可以实现叠掩等复杂场景的3维重建，弥补了常规InSAR技术的缺陷，拓展了SAR测绘技术的应用范围。

3.3 阵列干涉SAR技术特点

阵列干涉SAR技术利用阵列天线单次航过实现3维成像，解决了层析SAR观测周期长、下视阵列测绘效率低等问题，但是也面临3个核心技术难题。第一，阵列干涉SAR高程向分辨能力源自角度分辨，根据雷达分辨理论，分辨率与天线尺寸成反比，分辨率越高，天线尺寸越长，要实现1 m的3维成像分辨率，需要约20～50 m的机载雷达天线，工程上难以实现，成为制约高分辨率3维成像的核心难题；第二，阵列干涉SAR系统基于MIMO原理，为了增加等效通道数量，多个通道同时发射同时接收信号，多路信号之间会产生严重的干扰和混叠，传统正交编码方法无法有效抑制此干扰，也是制约阵列干涉SAR性能的瓶颈问题；第三，阵列干涉SAR 3维成像对相位精度要求高，需要阵列天线相对形变小于1 mm，而在航空条件下，受到飞机震颤以及侧风等影响，分布式阵列天线柔性形变量达到厘米量级，导致多通道信号之间的相参性被破坏，无法实现高精度3维成像。

为了解决上述问题，中科院电子所研究团队提出了系列解决方案。

针对阵列天线长度有限导致高程向分辨率低的问题，提出了阵列干涉3维超分辨成像方法。对叠掩问题进行了详细分析，根据连续地形叠掩场景的特点发明了一种基于曲线模型约束的超分辨方法。将连续自然地形表述为分段曲线模型，将传统基于相关匹配滤波的目标分辨成像问题，转化为曲线模型参数的最优估计问题[47]。利用分段曲线参数满足稀疏化条件，可实现超分辨参数估计的特点，通过求解阵列雷达观测方程，实现小尺寸天线条件下的3维超分辨成像。阵列干涉SAR 3维超分辨成像方法原理见图10。

具体实现上，首先提出了自适应分段曲线划分方法，根据雷达回波2维空间谱确定的地物分辨率，进行最优的分段曲线划分。进一步，由于叠掩地形曲线可以表示为距离r关于斜高s的函数，且曲线上的点有3个信息即散射系数幅度、相位以及坐标，提出了基于地形2阶导数最小化约束的阵列雷达观测模型，首次在观测模型中引入了连续地形空间相关性约束，优化目标函数为

$$\min\left(\left\|F(K_r,K_s)-\sum\sigma_i\mathrm{e}^{-\mathrm{j}(K_r r_i+K_s s_i-\phi_i)}\right\|_2^2+\lambda\left\|\Delta^2 r_i\right\|_2^2\right) \tag{3}$$

式(3)包含两层含义，一是求解的空间谱尽量接近测量值，二是使曲线尽量满足先验知识，即曲线尽量平滑，算法详细说明见文献[47]。通过在阵列干

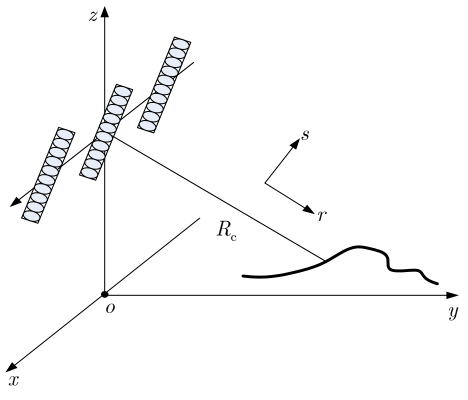

(a) 阵列干涉SAR几何关系图

(a) Array InSAR imaging geometry

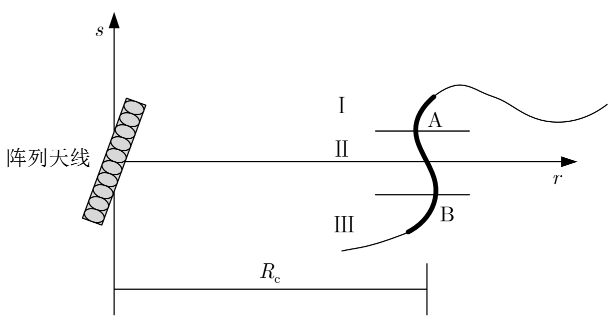

(b) 自适应分段曲线划分示意图

(b) Adaptive segmentation of curve model

图 10 阵列干涉SAR 3维超分辨成像算法原理示意图

Fig. 10 Diagrammatic sketch of Array InSAR super-resolution imaging algorithm

涉SAR观测模型中引入的连续地形空间相关性约束，结合最优化求解方法可以大幅提升3维分辨性能，相比传统方法，高程分辨率理论上可提高50倍，工程上提高了10～20倍。即采用2 m的天线，可获得20～40 m天线的分辨率。利用传统谱估计方法和阵列超分辨成像算法得到的3维成像结果对比见图11，从图11(b)和图11(c)的对比中可知，由于阵列天线尺寸受限，传统成像方法高程向分辨率低，阵列干涉超分辨算法则有效解决了这个问题，有效提升了3维成像质量。

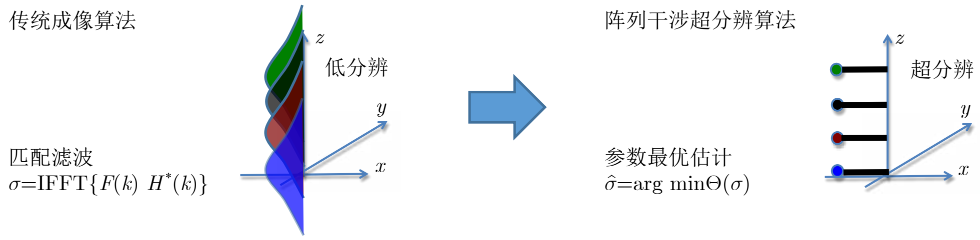

(a) 传统成像算法与阵列干涉超分辨算法原理对比
(a) Comparison of traditional imaging methods and Array InSAR super-resolution imaging algorithm

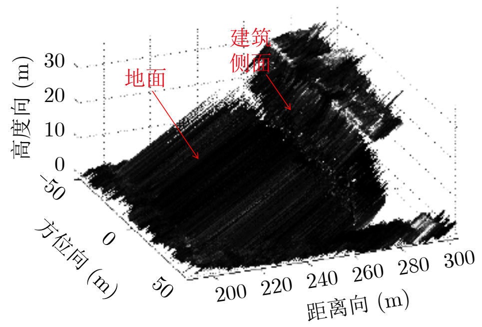

(b) 基于谱估计理论的3维成像结果
(b) 3D imaging resultsby spectral estimation

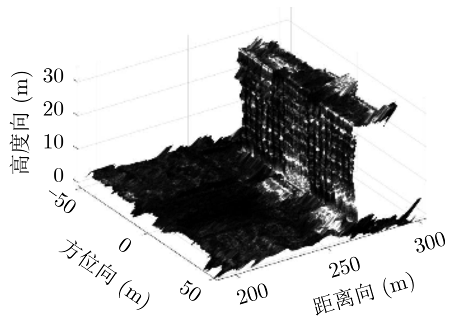

(c) 基于阵列超分辨算法的3维成像结果
(c) 3D imaging results by super-resolution algorithm

图 11 传统成像算法与阵列超分辨算法原理及效果对比

Fig. 11 Comparison of principles and performances between traditional methods and Array InSAR imaging method

针对阵列天线多通道信号之间干扰的问题，文献[49–52]提出了MIMO阵列雷达正交信号编码方法，在时频2维编码的基础上，利用阵列天线运动形成的空间维度，增加了空间相位编码，采用多维滤波模型，在空时频3维空间实现了多个混叠回波的解调分离(见图12)，将混叠抑制比从–10 dB提高到–38 dB，图像质量显著提高(如图13)。针对分布式阵列天线随飞机震颤产生弹性形变的问题，文献[53]发明了一种刚柔组合的柔性基线测量和补偿方法，原理见图14。首先用惯性测量系统实现1 cm精度的天线基线刚性段测量，据此反演出3维地形初值，并利用地面控制点计算出与实际高程的偏差，精密反演出惯性测量系统的内置误差，进一步利用多基线干涉模型精确反演出每个阵列节点的柔性形变量，最终能够实现优于1 mm的天线形变测量和补偿。

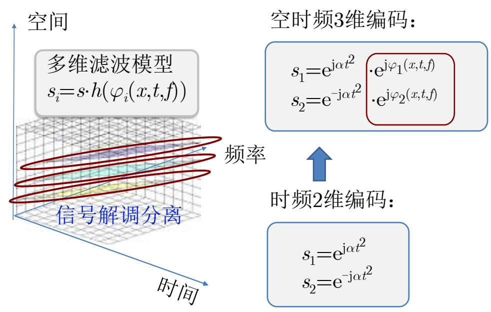

图 12 空时频多维信号波形编码方案原理示意图

Fig. 12 Diagrammatic sketch of multidimensional waveform coding

2015年，中科院电子所研制成功国际上第1部阵列干涉3维SAR系统，见图15。该机载雷达系统采用侧视工作模式，共10个阵元2发8收，跨航向形成16个通道，等效相位中心均匀分布。系统工作于Ku波段，采用调频连续波体制，发射信号带宽500 MHz，测绘带宽度达到34 km。同年，在山西地区开展了大量飞行试验，国际上首次实现了基于机载阵列的大面积复杂城市3维成像。图16展示了针对独栋建筑的阵列干涉SAR 3维重建结果。如图16所示，原始SAR图像中叠掩现象严重，地面、建筑侧面与顶面3个部分难以分辨，利用阵列干涉SAR 3维成像方法能够将叠掩的3部分进行区分，最终得到了基于建筑物3维模型约束的SAR 3维成

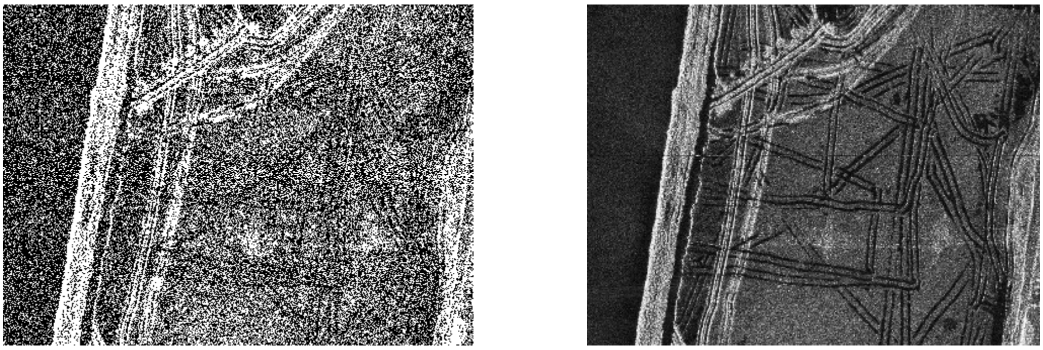

(a) 传统时频2维编码成像结果 (混叠抑制比-10 dB)
(a) Imaging result soft raditional waveform coding

(b) 多维信号波形正交编码成像结果 (混叠抑制比-38 dB)
(b) Imaging results of multidimensional orthogonal waveform

图 13 多维信号波形正交编码成像结果对比图

Fig. 13 Comparison between traditional and multidimensional orthogonal waveform imaging results

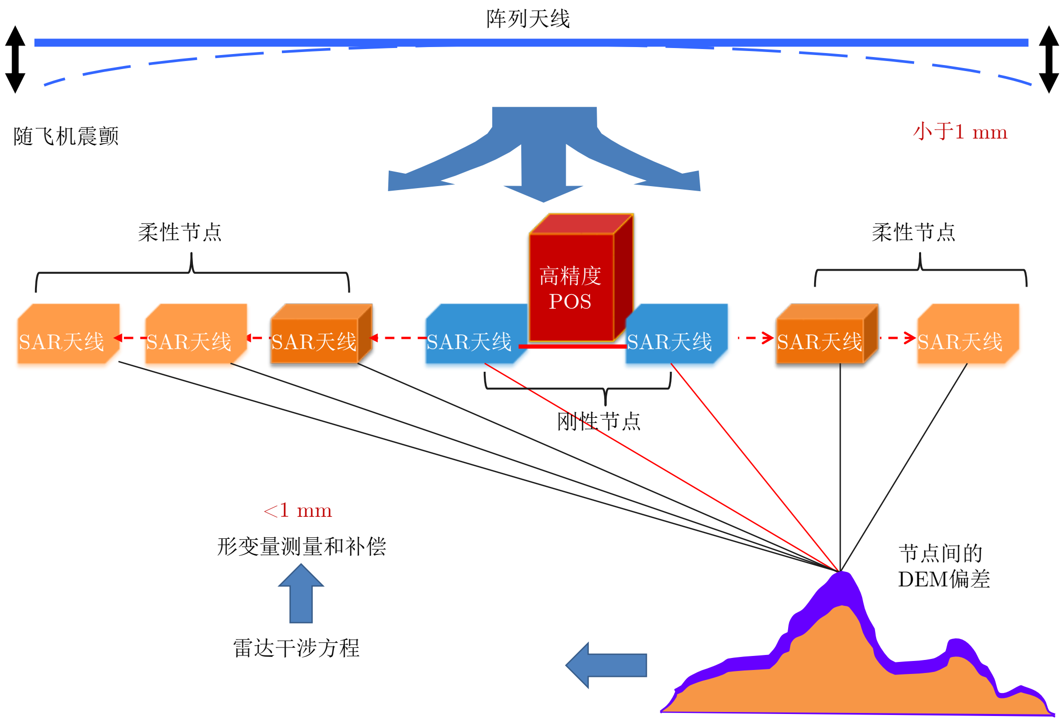

图 14 刚柔组合的柔性基线测量和补偿方法原理示意图

Fig. 14 Diagrammatic sketch of flexible baseline measurement and compensation algorithm

(a) 阵列干涉SAR机载平台
(a) Airplane of array InSAR

(b) 阵列天线 (2发8收)
(b) Linear array

(c) 舱内处理设备
(c) Processing center

图 15 中科院电子所阵列干涉SAR 3维成像系统

Fig. 15 Array InSAR 3D imaging system by IECAS

像结果。从该图中可以看到楼前地面的散射信息，楼前台阶、水泥路面，楼体侧面的纹理信息，窗户、玻璃幕墙和雨罩等结构，以及建筑的二面角反射等特征。图17则展示了整个小区的SAR图像以及阵列干涉SAR 3维成像结果，可以看出，小区3维结构清晰，证实了阵列干涉SAR的高精度城市3维成像能力。

4 SAR微波视觉3维成像技术

由上可见，目前国内外提出的TomoSAR以及阵列干涉SAR 3维成像技术体制，由于需要在高程向构建等效阵列，至少需要十余个飞行架次或天线阵列，导致在实际应用中，在轨卫星实现难、推广应用难、小型化难。因此，如何降低TomoSAR和阵列干涉SAR 3维成像所需阵列或重轨观测的数量，成为SAR 3维成像领域的核心难题。

为了解决上述问题，需要挖掘新的信息来源。实际上SAR 2维图像中蕴藏着3维信息，经过一定训练的SAR图像判读人员观察SAR图像能够很强烈的感知其中的3维信息，尤其对于SAR图像中建筑、桥梁等先验知识比较丰富的3维目标。此外，SAR回波散射机制中也蕴藏着3维信息，通过散射机制的提取和参数反演，具备对散射中心结构一定的判断能力。因此，本文提出能否将SAR 2维图像和回

(a) 建筑实景光学图像
(a) Optical image

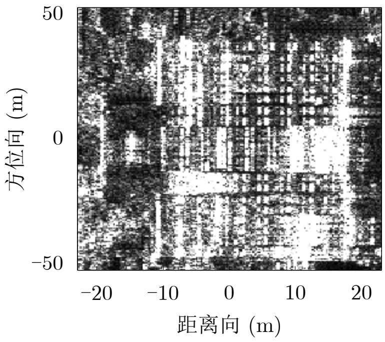

(b) 某通道SAR图像
(b) 2D SAR image

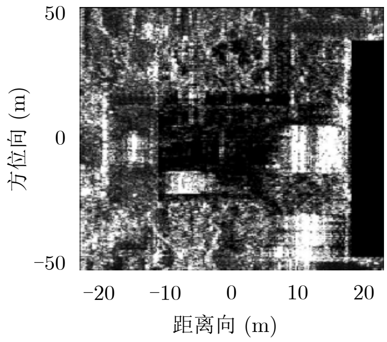

(c) 楼前地面SAR图像
(c) 2D image of the ground

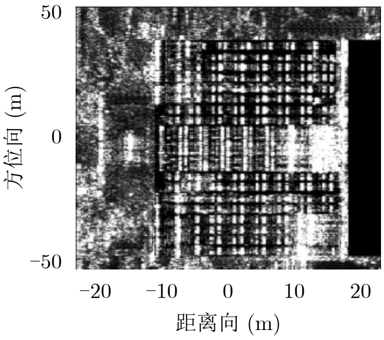

(d) 建筑侧面SAR图像
(d) 2D image of the facade

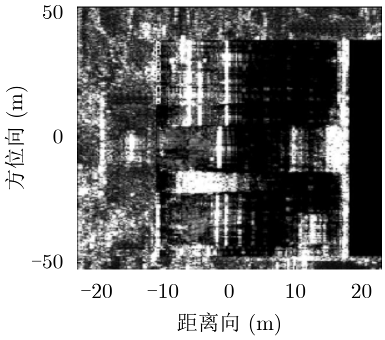

(e) 建筑顶面SAR图像
(e) 2D SAR image of the roof

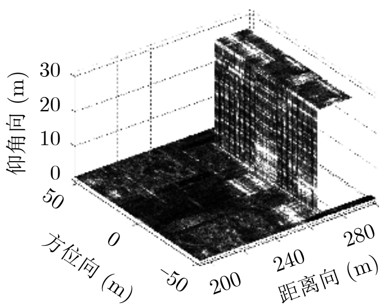

(f) 建筑物3维模型贴片结果
(f) 3D imaging results

图 16 独栋建筑阵列干涉SAR 3维成像结果

Fig. 16 Array InSAR 3D imaging results of a single building

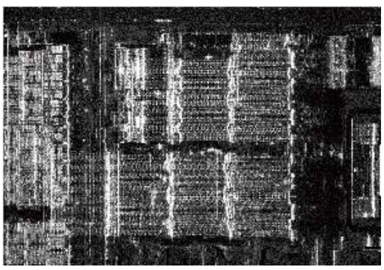

(a) 阵列干涉SAR系统某通道SAR图像
(a) SAR image of array InSAR system

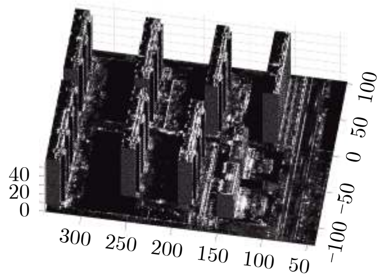

(b) 阵列干涉SAR 3维成像结果
(b) 3D imaging results by array InSAR

图 17 阵列干涉SAR小区场景3维重建结果

Fig. 17 3D imaging results by array InSAR of the observed scene

波信号中的信息充分挖掘提取，成为新的信息来源，与合成孔径雷达成像机理相结合，实现3维成像，同时降低对阵列通道数和重轨观测次数的需求。这便是本文提出的合成孔径雷达微波视觉3维成像的基本思路。

4.1 SAR微波视觉3维成像的概念

SAR微波视觉3维成像，是指将雷达回波和2维图像中隐含的3维线索，通过微波散射机制(微波)和图像视觉语义(视觉)挖掘的方法加以提取，并引入到传统的SAR成像方法中，从而降低所需多角度观测的数量，实现高效的3维成像技术。SAR微波视觉3维成像，融合了计算电磁学、计算机视觉以及雷达信号处理相关理论，是一种新的SAR 3维成像技术路线。

SAR微波视觉3维成像，相较传统3维成像方法，主要有以下特点。第一，SAR微波视觉3维成像方法从回波出发，建立目标部件3维结构和回波之间的3维散射映射关系，并构建目标3维散射机制的结构化参数表征，增加目标3维重建信息量。第二，现有SAR 3维成像方法逐像素孤立解算，而SAR微波视觉3维成像则结合计算机视觉方法提取图像中的语义信息对第3维重建增加约束，减少所需观测数。

SAR微波视觉3维成像技术与传统成像技术在信息来源、分辨机理等方面均有所不同，具体对比如表1所示。SAR的距离维分辨，分辨机理是时间分辨，信息来源是频率扩展，处理方法是脉冲压缩；方位维分辨机理是角度分辨，信息来源是空间扩展，处理方法是合成孔径；现有技术的高度维分辨，其机理也是角度分辨，信息来源是空间扩展，处理方法从根本上讲依然是合成孔径。本技术SAR微波视觉3维成像，信息来源引入了散射机制和视觉语义，处理方法是SAR微波视觉3维成像这一新手段。可见，该技术与现有技术有实质的不同，是一种全新的技术思路。

4.2 SAR微波视觉3维成像的核心科学问题

为了实现SAR微波视觉3维成像的目的，需要挖掘SAR回波及2维图像中所蕴藏的3维信息。针对上述目的，虽已有一些研究基础，包括基于SAR图像内容提取目标3维信息的方法[54–56]和基于SAR信号散射机制提取的目标3维信息反演方法[57–59]等，但上述方法仍有较大的局限性，难以满足复杂场景SAR微波视觉3维成像的需求。总结而言，作为一种全新的3维成像方法，SAR微波视觉3维成像需进行理论与方法的探索性研究，主要包括3个核心科学问题，分别是：微波3维散射机制及其逆问题，SAR图像视觉3维认知理论与方法，以及基于微波视觉的3维成像理论与方法。

(1) 微波3维散射机制及其逆问题

微波3维散射机制及其逆问题是要解决如何从SAR回波数据中识别出微波散射机制，从一定程度上重构目标3维认知参数的问题。根据散射机制反演目标结构是一个电磁散射的逆问题，如图18，由于实际目标的电磁散射机制复杂，目标散射特性及其在SAR图像的成像特性与其几何物理参数(外形、材质等)、波形参数(频率、极化等)、观测条件(角度、模式等)等多个因素相关，因此，电磁散射逆问题存在多解性、收敛性、鲁棒性等问题。

表 1 SAR 微波视觉3维成像与传统成像技术的对比

Tab. 1　Comparison between SAR microwave vision 3D imaging and traditional 3D imaging techniques

维度		分辨机理	分辨方法	信息来源	雷达体制
1	距离维	时间分辨	脉冲压缩	频率扩展	传统雷达
2	方位维	角度分辨	合成孔径	空间扩展	2维雷达成像(SAR)
3	高度维	角度分辨	合成孔径	空间扩展	层析/阵列干涉SAR 3维成像
		散射机制 视觉语义 角度分辨	SAR微波视觉 3维成像方法	散射机制 视觉内容 空间扩展	微波视觉 3维SAR

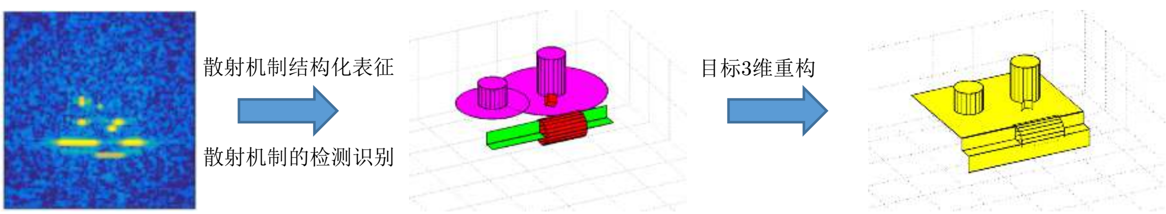

图 18 电磁散射求逆问题示意图

Fig. 18　Diagrammatic sketch of inverse problem of electromagnetic scattering

3维散射机制是目标微波视觉的重要信息，3维散射机制的识别是实现SAR微波视觉3维成像的核心科学问题之一，需要解决散射机制的检测识别、目标3维认知参数的反演与估计等理论方法问题[60,61]。

(2) SAR图像视觉3维认知理论与方法

SAR图像视觉3维认知理论与方法是解决如何理解SAR图像中的视觉语义并提取出典型目标的3维结构，挖掘出3维线索的问题。

针对光学图像，基于计算机视觉的图像理解和目标3维重建的研究已经比较成熟，已有研究可通过单幅光学影像进行3维重建[62]。但SAR与光学成像机理存在显著不同，如图19。首先SAR与光学的成像几何不同，光学是角度投影，有遮挡无叠掩、有角度信息无深度信息；而SAR是距离投影，有遮挡同时又有叠掩、无角度信息而有深度信息。第二，SAR与光学的电磁散射机理不同，光学是非相干成像，图像符合人眼视觉习惯，图像平滑、对观测角度不敏感，容易获取大量学习样本；而SAR是相干成像，图像相干斑噪声严重、随观测角度变化剧烈，很难获取大量学习样本，导致现有光学图像解译的方法应用于SAR图像视觉语义理解时，鲁棒性弱、泛化能力差等问题非常突出。因此，目前主要针对光学图像的计算机视觉理论方法无法直接照搬应用于SAR 图像视觉理解，需要创新性地发展SAR图像3维特征挖掘、目标表征和识别等理论方法，建立SAR 微波视觉3维成像的视觉认知基础。

(3) 基于微波视觉的3维成像理论与方法

基于微波视觉的3维成像理论与方法是要解决如何根据3维线索信息，高效精确地进行3维成像的问题，即：如何将微波散射机制和视觉语义与传统的SAR信号处理方法相结合，实现复杂环境和目标的3维成像，如图20。

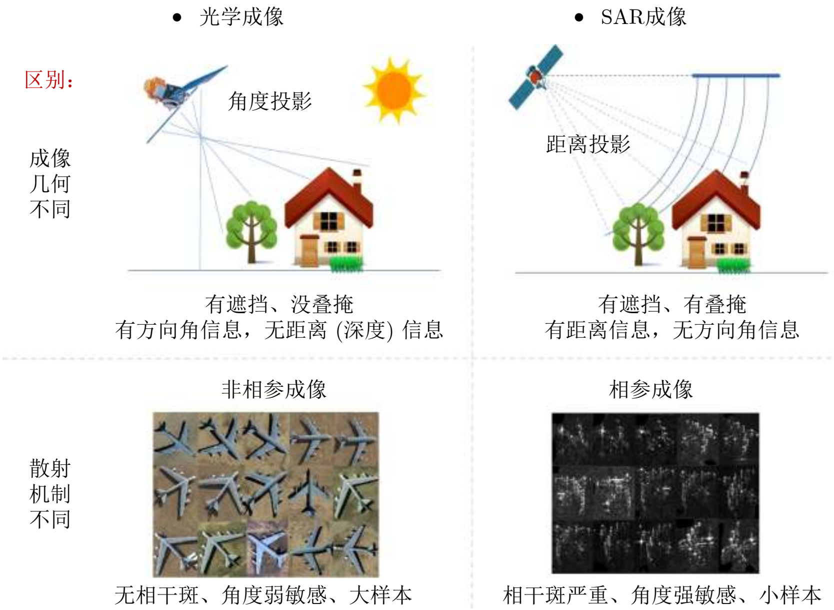

图 19 SAR成像与光学成像的区别

Fig. 19 Differences between SAR and optical images

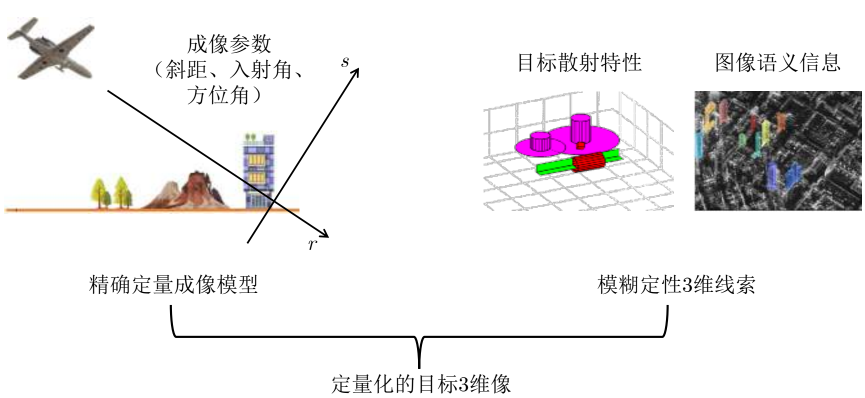

图 20 基于微波视觉的3维成像概念

Fig. 20 SAR microwave vision 3D imaging

通过“微波视觉”[63]一般获得的是异构、模糊、定性的3维线索，如何将异构定性的3维线索与定量化的SAR成像方法相结合，实现精确定量的3维成像，是必须解决的一个理论问题。现有SAR 3维成像技术需要大量多角度观测，核心原因是SAR图像方程中的高度维参数的解空间巨大，少数观测无法获得参数的唯一精确解。如果加入微波散射机制和图像视觉语义信息等约束条件，可有效缩小解空间范围，从而精确确定高度方向的各项参数，实现3维成像[64]。因此，需要创新构建SAR微波视觉3维成像理论框架，解决图像语义与微波散射机制的约束模型构建、异构非线性SAR 3维成像方程最优化求解等难题，发展基于微波视觉的3维成像理论与方法。

初步技术思路如下。根据SAR成像方程，如式(4)

$$\left\{\begin{aligned} &S_j(R_j,\eta_j)=\exp\left\{-\mathrm{j}\frac{4\pi R_j}{\lambda}\right\}\\ &\quad\cdot\sum_{i=1,2,\cdots,N}|\sigma_i(h_i|R_j,\eta_j)|\exp\{\mathrm{j}\phi_i\}\\ &\sqrt{\left(\sqrt{{R_j}^2-{h_i}^2}-X_j\right)^2+(h_i-H_j)^2}=R_j,\\ &\quad i=1,2,\cdots,N \end{aligned}\right. \tag{4}$$

该等式为某次观测下SAR图像方程中复数据表达式，其中R_j是斜距，η_j对应方位向慢时间，λ是雷达工作波长，σ_i对应等距圆弧上第i个散射中心对应的散射系数，ϕ_i为该散射系数的相位，h_i为该散射中心的高度，N为该等距圆弧上叠掩的散射中心的个数，如图21所示。

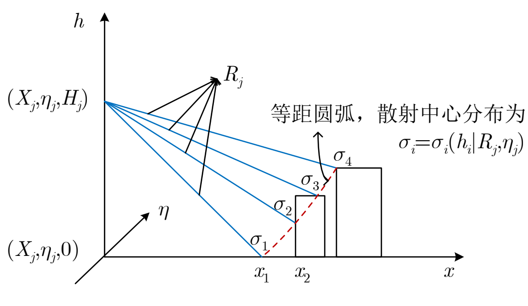

图 21 SAR图像中某叠掩像素的信号表达式

Fig. 21 Signal model of the overlapping pixel

在现有的稀疏3维成像算法中，对σ_i有稀疏性假设，但对σ_i和高程h_i没有约束条件，解空间很大，在少量观测下无法满足求解条件，故对多角度观测的数量有较高要求。本技术思路在综合考虑目标散射特性与SAR图像语义信息的情况下，引入视觉语义和散射机制的约束，缩小求解空间，如式(5)所示，

$$\left\{\begin{aligned} &h_i\in f(h,x)\\ &N\in\{K\},(|\sigma_i|,\phi_i)\in\{|\sigma_K|,\phi_K\} \end{aligned}\right. \tag{5}$$

其中，$h_i\in f(h,x)$表示根据微波视觉推断得到散射中心位于某条曲线上，$N\in\{K\}$表示叠掩的散射中心数量具有先验知识，$(|\sigma_i|,\phi_i)\in\{|\sigma_K|,\phi_K\}$表示散射中心的取值具有一定先验知识，通过联立上述方程组实现求解。此外，如微波视觉获得的约束无上述显式表达，还可基于散射机制和视觉语义中挖掘的目标几何基元对应像素间的连续性约束、待求参数符合一定先验分布等建立约束模型，采用多约束压缩感知以及深度神经网络来实现复杂多约束下逆问题的优化求解。

5　结束语

合成孔径雷达3维成像技术可以直接获得目标的3维电磁散射结构，在城市测绘和灾害评估等领域发挥了重大作用。本文回顾了合成孔径雷达3维成像技术的发展，详细介绍了TomoSAR以及阵列干涉SAR的技术体制和特点，指出现有3维成像技术受限于理论制约，系统复杂度高或成像周期长，限制了其大规模推广应用。

针对上述问题，本文提出了SAR微波视觉3维成像理论方法，针对现有3维成像方法中并未利用的微波散射机制、图像视觉语义等含有的3维信息，利用计算电磁学、计算机视觉等相关理论方法加以提取，并将其表达成对SAR信号处理的约束条件，实现3维信息的馈入，大大降低3维成像对空间扩展观测数量的依赖，最终实现少量观测下的SAR 3维成像，为SAR 3维成像技术发展开辟了新的方向。目前，SAR微波视觉3维成像的研究尚处于理论探索阶段，需要进一步开展相关研究，推进SAR 3维成像技术的发展。

参 考 文 献

[1] GRAHAM L C. Synthetic interferometer radar for topographic mapping[J]. *Proceedings of the IEEE*, 1974, 62(6): 763–768. doi: 10.1109/PROC.1974.9516.

[2] LAPRADE G L. An analytical and experimental study of stereo for radar[J]. *Photogrammetric Engineering*, 1963, 29(2): 294–300.

[3] LEBERL F W, RAGGAM J, and KOBRICK M. On stereo viewing of SAR images[J]. *IEEE Transactions on Geoscience and Remote Sensing*, 1985, GE-23(2): 110–117. doi: 10.1109/TGRS.1985.289407.

[4] KNAELL K. Three-dimensional SAR from curvilinear apertures[C]. Proceedings of the 1996 IEEE national Radar

Conference, Ann Arbor, USA, 1996.

[5] SCHMITT M and ZHU Xiaoxiang. Demonstration of single-pass millimeterwave SAR tomography for forest volumes[J]. *IEEE Geoscience and Remote Sensing Letters*, 2016, 13(2): 202–206. doi: 10.1109/LGRS.2015.2506150.

[6] ZHU Xiaoxiang and BAMLER R. Tomographic SAR inversion by L_1-norm regularization—the compressive sensing approach[J]. *IEEE Transactions on Geoscience and Remote Sensing*, 2010, 48(10): 3839–3846. doi: 10.1109/TGRS.2010.2048117.

[7] ZHU Xiaoxiang and BAMLER R. Very high resolution spaceborne SAR tomography in urban environment[J]. *IEEE Transactions on Geoscience and Remote Sensing*, 2010, 48(12): 4296–4308. doi: 10.1109/TGRS.2010.2050487.

[8] PASQUALI P, PRATI C, ROCCA F, *et al.* A 3-D sar experiment with EMSL data[C]. Proceedings of International Geoscience and Remote Sensing Symposium, IGARSS'95, Quantitative Remote Sensing for Science and Applications, Firenze, Italy, 1995: 784–786.

[9] REIGBER A and MOREIRA A. First demonstration of airborne SAR tomography using multibaseline L-band data[J]. *IEEE Transactions on Geoscience and Remote Sensing*, 2000, 38(5): 2142–2152. doi: 10.1109/36.868873.

[10] FORNARO G, LOMBARDINI F, and SERAFINO F. Three-dimensional multipass SAR focusing: Experiments with long-term spaceborne data[J]. *IEEE Transactions on Geoscience and Remote Sensing*, 2005, 43(4): 702–714. doi: 10.1109/TGRS.2005.843567.

[11] FORNARO G, LOMBARDINI F, PAUCIULLO A, *et al.* Tomographic processing of interferometric SAR data: Developments, applications, and future research perspectives[J]. *IEEE Signal Processing Magazine*, 2014, 31(4): 41–50. doi: 10.1109/MSP.2014.2312073.

[12] REALE D, FORNARO G, PAUCIULLO A, *et al.* Tomographic imaging and monitoring of buildings with very high resolution SAR data[J]. *IEEE Geoscience and Remote Sensing Letters*, 2011, 8(4): 661–665. doi: 10.1109/LGRS.2010.2098845.

[13] ZHU Xiaoxiang and BAMLER R. Demonstration of super-resolution for tomographic SAR imaging in urban environment[J]. *IEEE Transactions on Geoscience and Remote Sensing*, 2012, 50(8): 3150–3157. doi: 10.1109/TGRS.2011.2177843.

[14] ZHU Xiaoxiang, MONTAZERI S, GISINGER C, *et al.* Geodetic SAR tomography[J]. *IEEE Transactions on Geoscience and Remote Sensing*, 2016, 54(1): 18–35. doi: 10.1109/TGRS.2015.2448686.

[15] WANG Yuanyuan, ZHU Xiaoxiang, and BAMLER R. An efficient tomographic inversion approach for urban mapping using meter resolution SAR image stacks[J]. *IEEE Geoscience and Remote Sensing Letters*, 2014, 11(7): 1250–1254. doi: 10.1109/LGRS.2013.2290833.

[16] ZHU Xiaoxiang and BAMLER R. Super-resolution power and robustness of compressive sensing for spectral estimation with application to spaceborne tomographic SAR[J]. *IEEE Transactions on Geoscience and Remote Sensing*, 2011, 50(1): 247–258.

[17] ZHU Xiaoxiang and BAMLER R. Superresolving SAR tomography for multidimensional imaging of urban areas: Compressive sensing-based TomoSAR inversion[J]. *IEEE Signal Processing Magazine*, 2014, 31(4): 51–58. doi: 10.1109/MSP.2014.2312098.

[18] ZHU Xiaoxiang, GE Nan, and SHAHZAD M. Joint sparsity in SAR tomography for urban mapping[J]. *IEEE Journal of Selected Topics in Signal Processing*, 2015, 9(8): 1498–1509. doi: 10.1109/JSTSP.2015.2469646.

[19] TEBALDINI S and ROCCA F. Multibaseline polarimetric SAR tomography of a boreal forest at P-and L-bands[J]. *IEEE Transactions on Geoscience and Remote Sensing*, 2012, 50(1): 232–246. doi: 10.1109/TGRS.2011.2159614.

[20] PONCE O, PRATS-IRAOLA P, SCHEIBER R, *et al.* First airborne demonstration of holographic SAR tomography with fully Polarimetric multicircular acquisitions at L-Band[J]. *IEEE Transactions on Geoscience and Remote Sensing*, 2016, 54(10): 6170–6196. doi: 10.1109/TGRS.2016.2582959.

[21] BI Hui, ZHANG Bingchen, and HONG Wen. *Lq* regularization-based unobserved baselines' data estimation method for tomographic synthetic aperture radar inversion[J]. *Journal of Applied Remote Sensing*, 2016, 10(3): 035014. doi: 10.1117/1.JRS.10.035014.

[22] BI Hui, LIU Jianguo, ZHANG Bingchen, *et al.* Baseline distribution optimization and missing data completion in wavelet-based CS-TomoSAR[J]. *Science China Information Sciences*, 2018, 61(4): 042302. doi: 10.1007/s11432-016-9068-y.

[23] WEI Lianhuan, BALZ T, and LIAO Mingsheng. Tomographic analysis of high-rise buildings using TerraSAR-X spotlight data with compressive sensing approach[C]. Proceedings of 2014 IEEE Geoscience and Remote Sensing Symposium, Quebec City, Canada, 2014.

[24] WANG Jinfeng and PI Yiming. SAR tomography imaging via higher-order spectrum analysis[J]. *Journal of Systems Engineering and Electronics*, 2009, 20(4): 748–754.

[25] DONOHO D L. Compressed sensing[J]. *IEEE Transactions on Information Theory*, 2006, 52(4): 1289–1306. doi: 10.1109/TIT.2006.871582.

[26] BARANIUK R G. Compressive sensing[J]. *IEEE Signal Processing Magazine*, 2007, 24(4): 181–121.

[27] BARANIUK R and STEEGHS P. Compressive radar imaging[C]. Proceedings of 2007 IEEE Radar Conference,

Boston, USA, 2007: 128-133.

[28] BUDILLON A, EVANGELISTA A, and SCHIRINZI G. SAR tomography from sparse samples[C]. Proceedings of 2009 IEEE International Geoscience and Remote Sensing Symposium, Cape Town, South Africa, 2009: IV-865–IV-868.

[29] BUDILLON A, EVANGELISTA A, and SCHIRINZI G. Three-dimensional SAR focusing from multipass signals using compressive sampling[J]. *IEEE Transactions on Geoscience and Remote Sensing*, 2011, 49(1): 488–499. doi: 10.1109/TGRS.2010.2054099.

[30] REN X Z and SUN F. Tomography SAR imaging strategy based on block-sparse model[J]. *Progress in Electromagnetics Research M*, 2016, 47: 191–200. doi: 10.2528/PIERM16010904.

[31] WEI Lianhuan, BALZ T, ZHANG Lu, *et al*. A novel fast approach for SAR tomography: Two-step iterative shrinkage/thresholding[J]. *IEEE Geoscience and Remote Sensing Letters*, 2015, 12(6): 1377–1381. doi: 10.1109/LGRS.2015.2402124.

[32] SHI Yilei, ZHU Xiaoxiang, and BAMLER R. Nonlocal compressive sensing-based SAR tomography[J]. *IEEE Transactions on Geoscience and Remote Sensing*, 2019, 57(5): 3015–3024. doi: 10.1109/TGRS.2018.2879382.

[33] YOON Y T, EINEDER M, YAGUE-MARTINEZ N, *et al*. TerraSAR-X precise trajectory estimation and quality assessment[J]. *IEEE Transactions on Geoscience and Remote Sensing*, 2009, 47(6): 1859–1868. doi: 10.1109/TGRS.2008.2006983.

[34] DE FLORIO S and D'AMICO S. Optimal Autonomous Orbit Control of a Remote Sensing Spacecraft[M]. AAIA. Spaceflight Mechanics 2009. Univelt, San Diego: AAIA, 2009: 949-968.

[35] PITZ W and MILLER D. The TerraSAR-X satellite[J]. *IEEE Transactions on Geoscience and Remote Sensing*, 2010, 48(2): 615–622. doi: 10.1109/TGRS.2009.2037432.

[36] WERMUTH M, HAUSCHILD A, MONTENBRUCK O, *et al*. TerraSAR-X rapid and precise orbit determination[C]. Proceedings of the 21st International Symposium on Space Flight Dynamics, Toulouse, Frankreich, 2009.

[37] CALTAGIRONE F. Status, results and perspectives of the Italian Earth Observation SAR COSMO-SkyMed[C]. Proceedings of European Radar Conference, Rome, Italy, 2009: 330–334.

[38] GIERULL C H. On a concept for an airborne downward-looking imaging radar[J]. *International Journal of Electronics and Communications*, 1999, 53(6): 295–304.

[39] GIRET R, JEULAND H, and ENERT P. A study of a 3D-SAR concept for a millimeter wave imaging radar onboard an UAV[C]. The First European Radar Conference, Amsterdam, The Netherlands, 2004: 201–204.

[40] NOUVEL J, JEULAND H, BONIN G, *et al*. A Ka band imaging radar: DRIVE on board ONERA motorglider[C]. Proceedings of IEEE International Symposium on Geoscience and Remote Sensing, Denver, USA, 2006: 134–136.

[41] NOUVEL J F. ONERA DRIVE project[C]. Proceedings of International Radar Conference "Surveillance for a Safer World", Bordeaux, France, 2009: 1–4.

[42] WEIß M, PETERS O, and ENDER J. First flight trials with ARTINO[C]. Proceedings of the 7th European Conference on Synthetic Aperture Radar, Friedrichshafen, Germany, 2008: 1-4.

[43] KLARE J, BRENNER A, and ENDER J. Impact of platform attitude disturbances on the 3D imaging quality of the UAV ARTINO[C]. Proceedings of the 7th European Conference on Synthetic Aperture Radar, Friedrichshafen, Germany, 2008.

[44] WEIß M and GILLES M. Initial ARTINO radar experiments[C]. Proceedings of the 8th European Conference on Synthetic Aperture Radar, Aachen, Germany, 2010: 1–4.

[45] PENG Xueming, WANG Yanping, HONG Wen, *et al*. Airborne downward looking sparse linear array 3-D SAR heterogeneous parallel simulation[J]. *Remote Sensing*, 2013, 5(10): 5304–5329. doi: 10.3390/rs5105304.

[46] 彭学明, 王彦平, 谭维贤, 等. 基于跨航向稀疏阵列的机载下视MIMO 3D-SAR三维成像算法[J]. 电子与信息学报, 2012, 34(4): 943–949. doi: 10.3724/SP.J.1146.2011.00720.
PENG Xueming, WANG Yanping, TAN Weixian, *et al*. Airborne downward-looking MIMO 3D-SAR imaging algorithm based on cross-track thinned array[J]. *Journal of Electronics & Information Technology*, 2012, 34(4): 943–949. doi: 10.3724/SP.J.1146.2011.00720.

[47] ZHANG Fubo, LIANG Xingdong, WU Yirong, *et al*. 3D surface reconstruction of layover areas in continuous terrain for multi-baseline SAR interferometry using a curve model[J]. *International Journal of Remote Sensing*, 2015, 36(8): 2093–2112. doi: 10.1080/01431161.2015.1030042.

[48] LI Hang, LIANG Xingdong, ZHANG Fubo, *et al*. A novel 3-D reconstruction approach based on group sparsity of array InSAR[J]. *Scientia Sinica Informationis*, 2018, 48(8): 1051–1064. doi: 10.1360/N112017-00023.

[49] WANG Jie, LIANG Xingdong, and CHEN Longyong. MIMO SAR system using digital implemented OFDM waveforms[C]. Proceedings of IEEE International Geoscience and Remote Sensing Symposium, Munich, Germany, 2012: 7428–7431.

[50] WANG Jie, CHEN Longyong, LIANG Xingdong, *et al*. Implementation of the OFDM chirp waveform on MIMO SAR systems[J]. *IEEE Transactions on Geoscience and

Remote Sensing, 2015, 53(9): 5218–5228. doi: 10.1109/TGRS.2015.2419271.

[51] WANG Jie, LIANG Xingdong, DING Chibiao, *et al*. An improved OFDM chirp waveform used for MIMO SAR system[J]. *Science China Information Sciences*, 2014, 57(6): 1–9.

[52] 王杰, 丁赤飚, 梁兴东, 等. 机载同时同频MIMO-SAR系统研究概述[J]. 雷达学报, 2018, 7(2): 220–234. doi: 10.12000/JR17046.
WANG Jie, DING Chibiao, LIANG Xingdong, *et al*. Research outline of airborne MIMO-SAR system with same time-frequency coverage[J]. *Journal of Radars*, 2018, 7(2): 220–234. doi: 10.12000/JR17046.

[53] 向茂生, 丁赤飚. 一种基于刚性和柔性基线组合的多基线测量方法[P]. 中国, CN201210512927.4, 2014.

[54] SPORTOUCHE H, TUPIN F, and DENISE L. Extraction and three-dimensional reconstruction of isolated buildings in urban scenes from high-resolution optical and SAR Spaceborne images[J]. *IEEE Transactions on Geoscience and Remote Sensing*, 2011, 49(10): 3932–3946. doi: 10.1109/TGRS.2011.2132727.

[55] XU Feng and JIN Yaqiu. Automatic reconstruction of building objects from multiaspect meter-resolution SAR images[J]. *IEEE Transactions on Geoscience and Remote Sensing*, 2007, 45(7): 2336–2353. doi: 10.1109/TGRS.2007.896614.

[56] ZHANG Yueting, DING Chibiao, QIU Xiaolan, *et al*. The characteristics of the multipath scattering and the application for geometry extraction in high-resolution SAR images[J]. *IEEE Transactions on Geoscience and Remote Sensing*, 2015, 53(8): 4687–4699. doi: 10.1109/TGRS.2015.2406793.

[57] POTTER L C and MOSES R L. Attributed scattering centers for SAR ATR[J]. *IEEE Transactions on Image Processing*, 1997, 6(1): 79–91. doi: 10.1109/83.552098.

[58] JACKSON J A, RIGLING B D, and MOSES R L. Canonical scattering feature models for 3D and bistatic SAR[J]. *IEEE Transactions on Aerospace and Electronic Systems*, 2010, 46(2): 525–541. doi: 10.1109/TAES.2010.5461639.

[59] JACKSON J A and MOSES R L. Synthetic aperture radar 3D feature extraction for arbitrary flight paths[J]. *IEEE Transactions on Aerospace and Electronic Systems*, 2012, 48(3): 2065–2084. doi: 10.1109/TAES.2012.6237579.

[60] LI Yongchen, XU Feng, and JIN Yaqiu. A complex target reconstruction characterized by canonical scattering objects[C]. Proceedings of IEEE International Geoscience and Remote Sensing Symposium, Beijing, China, 2016: 1278–1280.

[61] XU Feng, JIN Yaqiu, and MOREIRA A. A preliminary study on SAR advanced information retrieval and scene reconstruction[J]. *IEEE Geoscience and Remote Sensing Letters*, 2016, 13(10): 1443–1447. doi: 10.1109/LGRS.2016.2590878.

[62] LIU Xiaobai, ZHAO Yibiao, and ZHU Songchun. Single-view 3D scene reconstruction and parsing by attribute grammar[J]. *IEEE Transactions on Pattern Analysis and Machine Intelligence*, 2018, 40(3): 710–725. doi: 10.1109/TPAMI.2017.2689007.

[63] 徐丰, 金亚秋. 从物理智能到微波视觉[J]. 科技导报, 2018, 36(10): 30–44.
XU Feng and JIN Yaqiu. From the emergence of intelligent science to the research of microwave vision[J]. *Science & Technology Review*, 2018, 36(10): 30–44.

[64] 陈健堃, 彭凌霄, 仇晓兰, 等. 基于深度神经网络的SAR建筑目标3维重建方法[J]. 中国科学: 信息科学, 2019, 49(11): 1–20.
CHEN Jiankun, PENG Lingxiao, QIU Xiaolan, *et al*. A 3D building reconstruction method for SAR based on deep neural network[J]. *Scientia Sinica Informationis*, 2019, 49(11): 1–20.

作 者 简 介

丁赤飚(1969–)，男，研究员，博士生导师，主要从事合成孔径雷达、遥感信息处理和应用系统等领域的研究工作，先后主持多项国家863重点项目和国家级遥感卫星地面系统工程建设项目，曾获国家科技进步一等奖、二等奖各一项。

仇晓兰(1982–)，女，中国科学院空天信息创新研究院研究员，博士生导师，主要研究领域为SAR成像处理、SAR图像理解，IEEE高级会员、IEEE地球科学与遥感快报副主编、雷达学报青年编委。

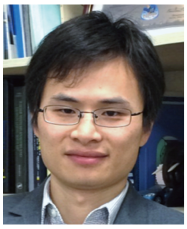

徐　丰(1982–)，男，复旦大学博士学位，教授，研究方向为SAR图像解译、电磁散射建模、人工智能。IEEE地球科学与遥感快报副主编、IEEE地球科学与遥感学会上海分会主席。

梁兴东(1973–)，男，陕西人，北京理工大学博士，中国科学院空天信息创新研究院研究员，研究方向为高分辨率合成孔径雷达系统、干涉合成孔径雷达、成像处理及应用、实时数字信号处理等。

焦泽坤(1991–)，男，博士，现任职于中国科学院空天信息创新研究院，助理研究员，研究方向为SAR 3维成像技术。

张福博(1988–)，男，副研究员，2015年获得工学博士学位，2016年入选中国科学院电子学研究所优秀人才计划，主要研究方向为微波3维成像技术，解决了超分辨和高相参信号处理难题，发表学术论文十余篇，获得2018年度国家技术发明奖。

Synthetic Aperture Radar Three-Dimensional Imaging——From TomoSAR and Array InSAR to Microwave Vision

DING Chibiao①②④ QIU Xiaolan*①③④ XU Feng⑤ LIANG Xingdong①②④
JIAO Zekun①② ZHANG Fubo①②④

①(*Aerospace Information Research Institute, Chinese Academy of Sciences, Beijing* 100190, *China*)

②(*National Key Lab of Microwave Imaging Technology, Beijing* 100190, *China*)

③(*Key Laboratory of Technology in Geo-spatial Information Processing and Application System, Beijing* 100190, *China*)

④(*University of Chinese Academy of Sciences, Beijing* 100049, *China*)

⑤(*Fudan University, Shanghai* 200433, *China*)

Abstract: Synthetic Aperture Radar three-dimensional (SAR 3D) imaging technology can eliminate severe overlap in 2D images, and improve target recognition and 3D modeling capabilities, which have become an important trend in SAR development. After decades of development of SAR 3D imaging technology, many types of 3D imaging methods have been proposed. In this study, the history of SAR 3D imaging technology is systematically reviewed and the characteristics of existing SAR 3D imaging technology are analyzed. Given that the 3D information contained in SAR echo and images is not fully used by existing techniques, a new concept of SAR microwave vision 3D imaging has been proposed for the first time. This new concept is integrated with microwave scattering mechanism and image visual semantics to realize three-dimensional reconstruction, which form the theory and method of SAR microwave vision 3D imaging and can achieve high-efficiency and low-cost SAR 3D imaging. This study also analyzes the concept, goal and key scientific problems of SAR microwave vision 3D imaging and provides a preliminary solution, which will contribute in several ways to our understanding of SAR 3D imaging and provide the basis for further research.

Key words: SAR 3D imaging; Array InSAR; SAR Tomography; SAR microwave vision 3D imaging

CLC index: TN957.52 **Document code**: A **Article number**: 2095-283X(2019)06-0693-17

DOI: 10.12000/JR19090

Reference format: DING Chibiao, QIU Xiaolan, XU Feng, *et al*. Synthetic aperture radar three-dimensional imaging ——from TomoSAR and array InSAR to microwave vision[J[J]. *Journal of Radars*, 2019, 8(6): 693–709. DOI: 10.12000/JR19090.

1 Introduction

Synthetic Aperture Radar (SAR) microwave imaging technology is an important means of high-resolution ground observation with great potential in military reconnaissance, topographic mapping, environmental monitoring, geological exploration, and disaster investigation. However, due to the significantly different mechanisms of SAR and optical imaging, SAR target recognition and image interpretation are extremely difficult, restricting the widespread use of current spaceborne and airborne SAR systems. The main reason is that the traditional SAR can only obtain 2D images. 3D targets in areas with steep terrain change and complex infrastructures will introduce severe overlap of the 2D SAR images. SAR 3D imaging can obtain the 3D electromagnetic scattering of the target structure directly, and eliminate the phenomena of contraction, overlap, and inversion of the top and bottom, which is of great significance to the application of 3D environment construction, target interpretation, urban mapping, and disaster assessment.

Manuscript received September 30, 2019; Revised November 04, 2019; Published online November 25, 2019.

*Communication author: QIU Xiaolan

E-mail: xlqiu@mail.ie.ac.cn

Foundation Items: Major Program of National Natural Science Foundation of China “Research on SAR Microwave Vision Three-Dimensional Imaging Theory and Application Foundation” (61991420, 61991421)

Corresponding Editor: ZHANG Qun

In this context, SAR 3D imaging technology has received great attention from various countries, leading to significant progress. Depending on whether the technology has 3D resolution, the development of SAR imaging from 2D to 3D can be roughly divided into two periods. The first started in the 1960s, which includes the interferometric synthetic aperture radar[1] (InSAR) and StereoSAR[2,3] to obtain 3D scene information. However, both the InSAR and StereoSAR technologies essentially used observations from different angles to extract the 3D position of the registered pixels. When overlap of multiple scatterers occurred, only the position of the synthetic scattering center can be solved. Therefore, only 3D surface information can be obtained, and 3D resolution is not available with these two techniques. The second period started in the 1990s. In 1995, K. K. Knaell and G. P. Cardillo[4] of the U.S. Naval Research Laboratory first proposed the concept of 3D SAR, and the technical idea of using a 3D synthetic aperture to realize 3D imaging. After that, research on SAR 3D imaging was performed around the world[5–11]. Currently, two SAR 3D imaging technologies are mainly used, *i.e.*, SAR Tomography (TomoSAR) and array interference SAR 3D imaging technology (array InSAR). These 3D imaging technologies both form a synthetic aperture in the elevation direction through multiple angle observations by multiple antennas to obtain the 3D resolution. However, these two methods require a large number of multi-angle observations, which leads to a long imaging period and highly complicated systems, preventing them from wide application.

Based on the development of SAR 3D imaging technology, from the early interferometric SAR technology to the current TomoSAR 3D imaging technology, the 3D position of the target is calculated via the radar imaging geometry combined with multi-angle observations. However, there are 3D clues in the SAR image such as the structure of the scene and the target, texture, and occlusion relations which have not been fully investigated in the current 3D imaging methods. This paper proposes a new SAR 3D imaging technology, *i.e.*, SAR microwave vision 3D imaging. Through investigation into the microwave scattering mechanism and image visual semantics, the 3D information contained in the radar echo and 2D images are extracted. Combined with the traditional SAR imaging theory, efficient SAR 3D imaging can be achieved, which will greatly reduce the number of observations required.

The remainder of this paper are organized as follows. In Sections 2 and Sections 3, the basic principles, technical characteristics and limitations of the current SAR 3D imaging technologies are analyzed. On this basis, the SAR microwave vision 3D imaging technology is proposed in Section 4. The concept, connotation and key scientific issues of the SAR microwave vision 3D imaging technology are introduced in detail, and preliminary approaches are given. Conclusions are drawn in Section 5.

2 TomoSAR 3D Imaging

2.1 Principle of TomoSAR 3D imaging

For the 3D reconstruction of complex scenes, such as urban areas with severe overlap, various studies are performed by institutions all over the world. Inspired by the medical Computed Tomography imaging technology, SAR Tomography (TomoSAR) 3D imaging technology is proposed. The principle of TomoSAR 3D imaging is presented in Fig. 1.

The 3D resolution ability of TomoSAR is presented in Fig. 1. Similar to traditional 2D SAR imaging, the range resolution is realized by transmitting a large bandwidth signal combined with the pulse compression technology, and the azimuth resolution is obtained by synthetic aperture. In the elevation direction, an equivalent array is constructed using multiple observations, of which the tracks are accurately controlled and meet the

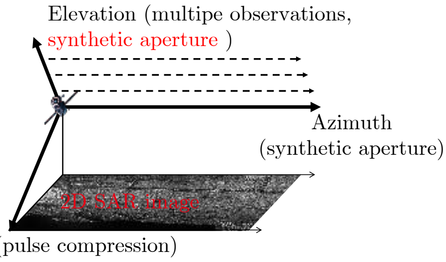

Fig. 1 Diagram of the TomoSAR 3D imaging

Nyquist Sampling Law to achieve synthetic aperture and obtain the resolution in the elevation direction. The geometry of TomoSAR 3D imaging is shown in Fig. 2[7]. First, a stack of SAR images with nearly the same incidence angle are registered. Then, the reflection profile in the elevation direction is reconstructed pixel by pixel.

Consider that there are N images in total, the complex value of pixels of the nth SAR image is as follows[6]

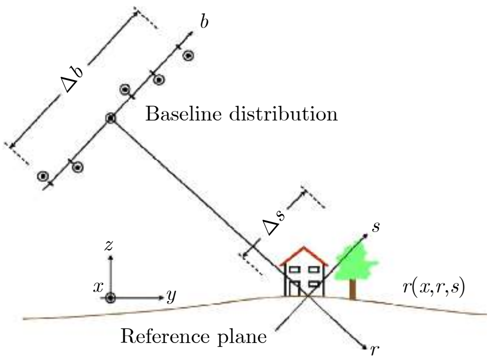

Fig. 2 TomoSAR imaging geometry

$$y_n = \int_{\Delta s} \gamma(s) \exp\left[-\mathrm{j}\frac{4\pi}{\lambda} R_n(s)\right] \mathrm{d}s \tag{1}$$

For the same pixel, the measurement vector $\boldsymbol{y}$ is formed using a stack of SAR images. After discretization in the elevation direction, the measurement equation can be expressed as:

$$\boldsymbol{y} = \boldsymbol{\Phi\gamma}+\boldsymbol{n} \tag{2}$$

in which $\boldsymbol{\Phi}_{i,j} = \exp(-\mathrm{j}4\pi/\lambda \cdot \Delta b_i s_j / R_0)$. By solving the inverse problem of Eq. (2), the reflection profile in the elevation direction can be obtained.

2.2 Research status of TomoSAR 3D imaging

The research of TomoSAR 3D imaging started in the mid-1990s, and its development has gone through three stages: laboratory research, airborne SAR tomography and spaceborne SAR tomography. In 1995, Pasquali *et al.* from European Microwave Signal Laboratory (EMSL)[8] proved for the first time that it is feasible to obtain resolution using a synthetic aperture in the elevation direction with multiple observations. The laboratory designed a Ku-band radar system with eight baselines, and two layers of metal spheres hidden in the medium were successfully distinguished in the elevation direction, which is the first demonstration of the TomoSAR 3D imaging technology. In 1998, Reigber *et al.* from Deutsches Zentrum für Luft- und Raumfahrt (DLR)[9] conducted research on airborne SAR tomography. L-band airborne SAR measured data was used to reconstruct the 3D structure of buildings and vegetation, which is the first airborne TomoSAR 3D imaging results. In 2005, Fornaro *et al.* from the University of Naples[10] used 30 SAR images of Naples acquired by the European Remote Sensing Satellite (ERS) from 1992 to 1998, and achieved spaceborne TomoSAR 3D imaging for the first time. In 2007, the German TerraSAR-X (TSX) satellite was launched. The satellite has good orbit control capability and extremely high phase measurement accuracy. The SAR image resolution can reach 1 m under the spotlight mode, which further promoted the development of the TomoSAR technology. In 2010, Xiaoxiang Zhu *et al.*[12] from DLR obtained TomoSAR 3D imaging results of complex urban scenes for the first time using TerraSAR-X data. The TomoSAR 3D imaging result of Las Vegas is shown in Fig. 3. The team then used the satellite data to conduct more spaceborne TomoSAR research, and achieved rich results regarding the tomographic SAR 3D imaging algorithm[13–18].

With the application of more fully polarized spaceborne and airborne SAR systems, Polarimetric TomoSAR (PolTomoSAR) technology emerges and plays a significant role in applications such as forest biomass inversion[19]. In the framework of traditional TomoSAR imaging, the incidence angle of different observations are nearly the same, tomographic imaging of shadow areas of the SAR image cannot be realized. To solve this problem, research on airborne SAR Holography (HoloSAR) imaging technologies have been conducted, which can realize 3D imaging which makes use of observations from all azimuth directions[20]. Some PolTomoSAR and HoloSAR results are presented in Fig. 4. Research on the TomoSAR technology have also been performed in China. The Institute of Electronics, Chinese Academy of Sciences (IECAS), Wuhan University, University of Electronic Science and Technology of

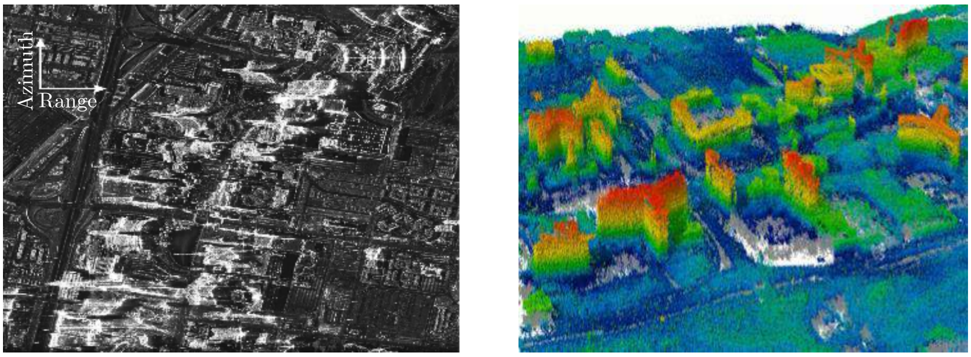

(a) TerraSAR-X radar image of LasVegas (b) TomoSAR 3D point cloud of LasVegas

Fig. 3 TomoSAR 3D imaging result of urban areas by DLR[12]

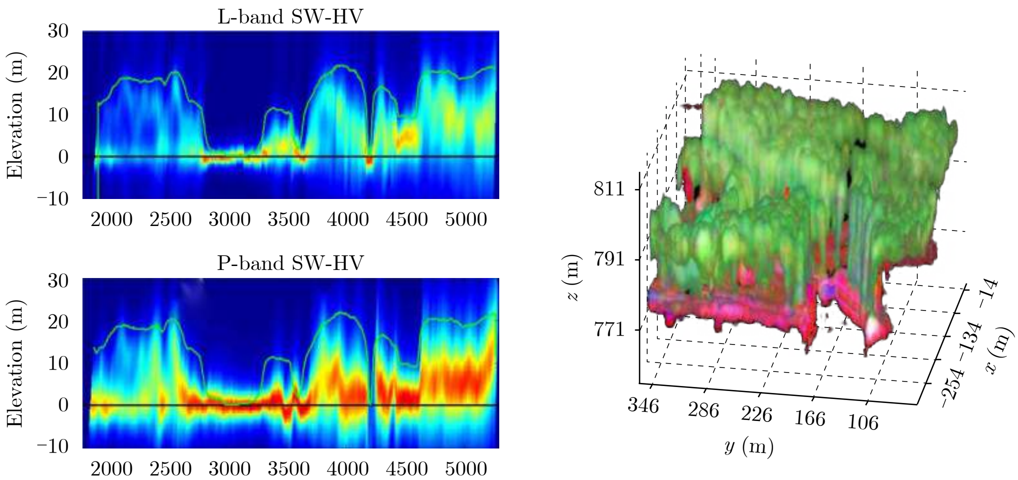

(a) PolTomoSAR 3D imaging results[19] (b) HoloSAR 3D imaging results of forest[20]

Fig. 4 Three-dimensional PolTomoSAR and HoloSAR imaging results

China[21–24] have achieved rich results regarding TomoSAR imaging algorithms.

2.3 Technical characteristics of TomoSAR

TomoSAR 3D imaging technology has achieved great success in 3D reconstruction in complex urban areas. However, there are two main difficulties in practical applications. First, the use of traditional signal processing methods, such as matched filtering, spectral estimation, require dozens, or even hundreds of flights with a long imaging period and high costs, which make it not applicable in applications with high timeliness requirements. Second, in order to ensure the coherence of SAR images of repeated orbit observations, accurate control of the trajectory is needed, which increases the difficulty of implementation.

Considering that TomoSAR 3D imaging method processes each pixel of the SAR image independently and the ground objects are sparsely distributed in the elevation direction, Compressed Sensing (CS) theory provides a solution for the first problem. In 2006, the theory of CS proposed by Donoho *et al.*[25] breaks through the limitation of Nyquist Sampling Law and can use a few observations to reconstruct the original signal with high probability under the sparsity hypothesis. In 2007, Baraniuk *et al.* proposed to adopt CS in the radar imaging[26,27]。In 2009, Alessandra Budillion *et al.*[28,29] from Italy conducted a TomoSAR simulation experiment based on CS theory. Notably, the CS technique can reduce the number of observations required for 3D reconstruction of the target. The technology was then applied to the ERS satellite data to successfully achieve 3D imaging of the buildings. In the same year, Xiaoxiang Zhu[16] from DLR applied the CS theory to high-resolution images of TerraSAR-X and obtained tomographic results of TerraSAR measured data. In 2011, the team proposed the SLIMMER algorithm and systematically analyzed its performance. In recent years, researchers around the world carried out a lot of research on tomography combined with CS theory, and obtained fruitful results in sparse imaging algorithms[17,18,30–32]. Fig. 5 illustrates the 3D imaging results with traditional and sparse observations. There is little difference between the results of seven images and 64 images, which proves the feasibility of the sparse observation in TomoSAR 3D imaging.

In order to ensure coherence between the repeated observation SAR images, the TomoSAR repeated orbit observations need to have a short baseline to avoid spatial decorrelation, which puts forward a high requirement for the orbit control accuracy. With the advancement of satellite orbit control technology, the accuracy of satellite orbit control, such as TerraSAR-X, has increased. For example, compared with the reference track, the orbit control accuracy of TerraSAR-X is better than 500 m, *i.e.*, all tracks are controlled in a pipe with a radius of about 250 m around the reference track as the axis, as shown in Fig. 6. Especially in the radial direction, the accuracy of repeating orbit control is better than 100 m[33], and the track measurement accuracy is better than a decimeter. The orbit control and measurement accuracy of the high-resolution spaceborne SAR systems, such as TerraSAR-X and Cosmo-Skymed, is sufficient for TomoSAR 3D imaging[33–37]. In con-

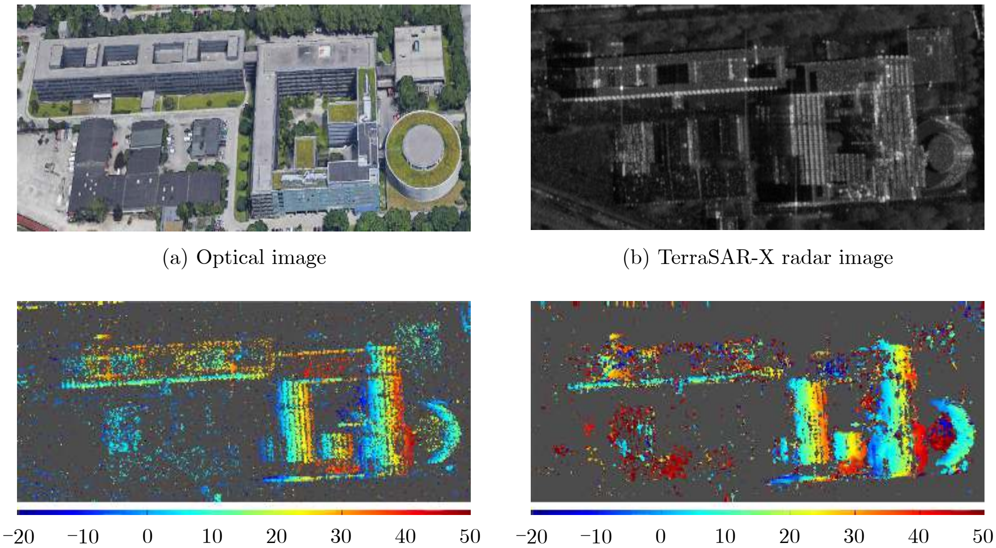

(a) Optical image

(b) TerraSAR-X radar image

(c) TomoSAR results with 64 images

(d) TomoSAR results with seven images

Fig. 5 TomoSAR imaging results of the DB Headquarters in Munich[32]

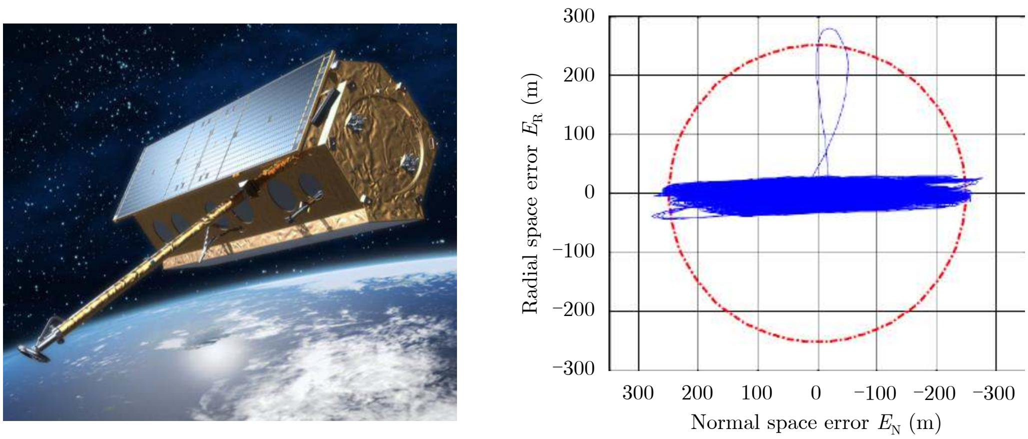

(a) TerraSAR-X satellite

(b) TSX orbit control performance during 4th quarter of 2009

Fig. 6 Diagram of the TSX orbit control performance[33] clusion, the orbit control accuracy of spaceborne SAR is sufficient for TomoSAR processing. However, it is very difficult to obtain effective airborne TomoSAR data because the system is easily affected by airflow.

Overall, the current TomoSAR 3D imaging process still requires more than ten repeated observations with strict orbit control and a long time span. These characteristics make it difficult to meet the timeliness requirement in many applications.

3 Array InSAR 3D imaging

3.1 Downward-looking array 3D imaging

Downward-looking array 3D imaging is a SAR 3D imaging technology based on array antennas. By deploying array antennas in a cross-track direction, 3D imaging of the scene directly below the aircraft can be achieved. A schematic diagram of the downward-looking array 3D imaging technology is shown in Fig. 7.

A downward-looking array 3D imaging system transmits a wideband signal directly below the aircraft. Combined with pulse compression technology, elevation resolution is achieved. In the azimuth direction, platform movement is used to form a synthetic aperture and obtain Doppler information to achieve azimuth resolution. In the cross-track direction, an array antenna is used to realize the cross-track synthetic aperture, which provides the cross-heading resolution.

In 1999, the concept of 2D downward-looking imaging radar was first proposed by DLR[38]. In 2004, Giret *et al.*[39] from ONERA proposed the concept of downward-looking array 3D imaging, which combines the array technique and SAR, realizing resolution ability in all three directions. The group then started to develop the corresponding downward-looking array 3D imaging system DRIVE. The system has two working modes, downward-looking 3D and side-looking 2D. The carrier is a glider with a wingspan of 23 m and a weight of 900 kg[40]. Between 2006 and 2010, Nouvel *et al.*[41] conducted downward-looking array imaging experiments with the DRIVE system, and the azimuth-elevation 2D imaging results were disclosed (Fig. 8). The azimuth span is 1 km, while the cross-track span is 42 m. Klare *et al.*[42,43] from FGAN-FHR began to develop the unmanned aerial array 3D SAR system ARTINO in 2005, with a wingspan of 4 m and a weight of 25 kg. In 2010, a flight experiment was performed on the calibration points, but the 3D imaging results were not published[44]. IECAS and UESTC in China[45,46] conducted research on downward-looking array 3D imaging, and has achieved rich results in imaging algorithm and experimental systems.

However, the downward-looking array SAR is limited by the imaging mechanism and has the following problems. First, the mapping swath is generally narrow. For example, the DRIVE system's cross-track mapping swath is only 42 m, leading to low work efficiency. Second, the downward-looking array SAR imaging system realizes resolution in the cross-track direction using a real aperture. The system needs to have a large number of channels in order to resolve the contradiction between resolution and swath, which cause the system to have higher complexity and cost. Finally, because of the downward-looking mode and limitations in the length of the array antenna, its cross-track resolution is low, which will lead to low density of the 3D point cloud and poor 3D imaging performance. So far, results by downward-looking array 3D imaging system have not been publicly published at home and abroad.

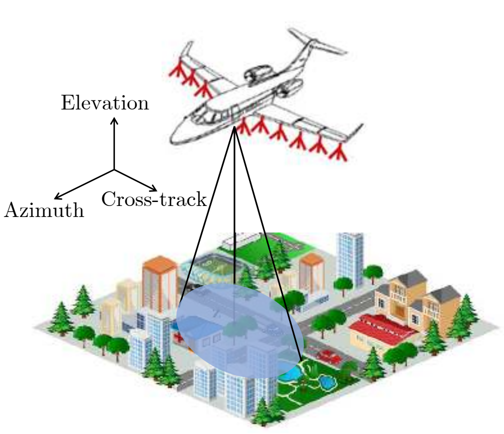

Fig. 7 Diagram of the downward-looking array 3D imaging

3.2 Array InSAR 3D imaging system

To address the problems of the downward-looking array 3D imaging, IECAS proposed the

(a) Diagram of ARTINO[42]

(b) Multi-Input Multi-Output (MIMO) antenna array of ARTINO[43]

(c) ONERA BUSARD motorglider[40]

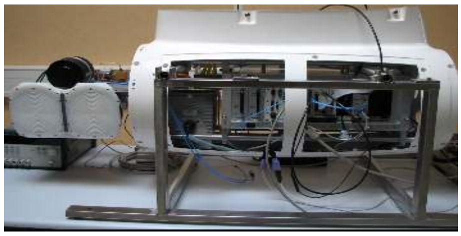

(d) Ka radar system of DRIVE[40]

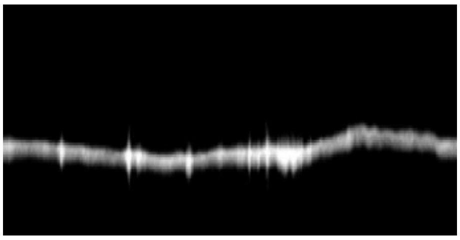

(e) Imaging result of DRIVE in the azimuth-elevation plane[41]

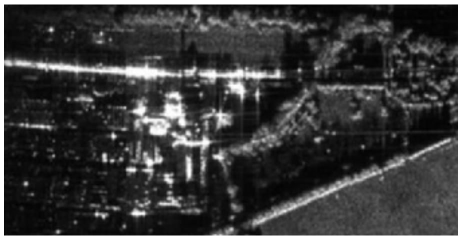

(f) 2D SAR image of the same area

Fig. 8　Global array 3D imaging systems

array InSAR technology that is used under side-looking imaging mode. A cross-track array antenna is used to virtualize multiple equivalent Antenna Phase Centers (APCs) based on the Multi-Input Multi-Output (MIMO) technology. Multi-channel SAR images are obtained and 3D imaging results are obtained in a single flight, with good coherence and timeliness. Compared with the downward-looking array 3D imaging technology, the array InSAR 3D imaging adopts the side-looking imaging mode, which leads to a larger mapping swath. The number of equivalent phase centers is much smaller than that of the downward-looking array system. The system complexity is lower with better stability and feasibility. The resolution in the range direction is better and the density of the reconstructed point clouds is greater, which will lead to a relatively good 3D imaging performance. The principle of the array InSAR 3D imaging is shown in Fig. 9.

The IECAS[47,48] began to develop the array InSAR system in 2005. A rigid antenna array with a length of 2 m and a weight of 150 kg is used to ensure the stability of the baseline. The baseline is measured based on the millimeter-level high-precision calibration and the multi-channel images are registered with high accuracy. A pixel by pixel 3D imaging method is adopted and the world's first 3D scene imaging results are obtained in 2015. The system combines the advantages of the high-resolution multi-channel array and high-precision coherent measurement. The system realizes the 3D reconstruction of complex scenes such as layover areas, which addresses the shortcomings of the conventional InSAR techno-

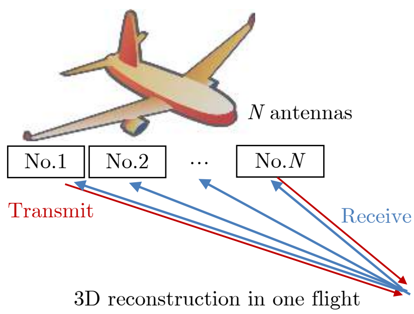

Fig. 9　Diagram of the array InSAR 3D imaging

logy and expands the application range of the SAR mapping technology.

3.3 Technical characteristics of the array InSAR

Array InSAR technology uses an antenna array to achieve 3D imaging in a single pass. It solves the problems of the long observation period in TomoSAR and low mapping efficiency of the downward-looking array 3D imaging. However, TomoSAR also has three core technical problems. First, the resolution capability of the array InSAR is based on angular resolution. According to radar resolution theory, the resolution is inversely proportional to the antenna size: the better the resolution, the longer the antenna size. To achieve 1 m 3D imaging resolution, an antenna array with length about 20 to 50 m is required, which is difficult to implement in engineering and becomes the core problem that restricts high-resolution 3D imaging. Second, the array InSAR system is based on the MIMO principle. When multiple channels transmits and receives signals at the same time, there will be serious interference and aliasing between multi-channel signals. Traditional orthogonal coding methods cannot effectively suppress this interference, which is also a bottleneck problem that restricts the performance of the array InSAR. Third, the phase measurement accuracy requirements of array InSAR 3D imaging are very high; the relative deformation of the array antenna typically need to be less than 1 mm. In an airborne system, due to aircraft tremors and crosswind, the flexible deformation of the distributed array antenna is on the order of centimeters, which leads to the destroyed coherence between the multi-channel images and failure of the high-precision 3D imaging.

In order to solve the above problems, the research team of the IECAS proposed a series of solutions.

To address the low resolution in the elevation direction due to the limited array antenna length, an array InSAR 3D super-resolution imaging method was proposed. The layover problem is analyzed in detail, and a super-resolution method based on the constraints of the curve model was proposed according to the characteristics of the continuous layover scenario. The continuous natural terrain is expressed as a piecewise curve model, and the traditional imaging problem based on matched filtering is transformed into an optimal estimation problem of the curve model parameters[47]. If the parameters of the segmented curve model satisfy the sparse conditions, super-resolution parameter estimation can be achieved. By solving the observation equation of the radar array, the 3D super-resolution imaging with a small antenna can be realized. The principle of a 3D super-resolution imaging method for the array InSAR is shown in Fig. 10.

In the specific implementation, an adaptive segmentation curve division method is first proposed, and the optimal curve segmentation is performed according to the resolution determined by the 2D spatial spectrum of the radar echo. An observation model based on the minimization constraints of the terrain's second derivative is proposed considering the layover terrain curve can be expressed as a function of the distance r with re-

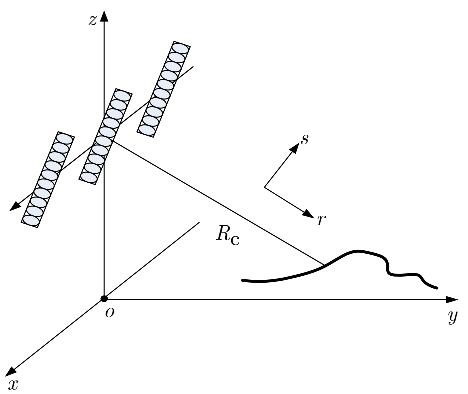

(a) Array InSAR imaging geometry

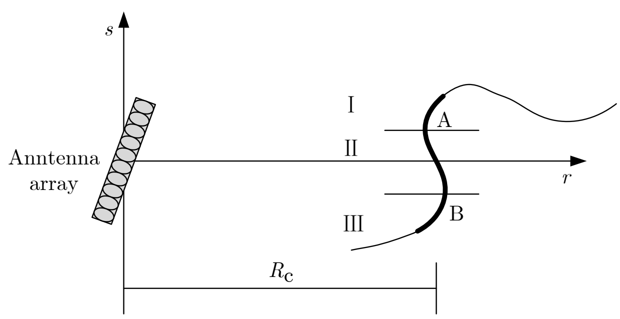

(b) Adaptive segmentation of curve model

Fig. 10 Diagram of the array InSAR super-resolution imaging algorithm spect to the elevation s, and the points on the curve have three pieces of information, the scattering coefficient amplitude, phase, and coordinates. Continuous terrain spatial correlation constraints are introduced into the observation model for the first time. The optimization objective function is as follows:

$$\min\left(\left\|F(K_r,K_s)-\sum\sigma_i \mathrm{e}^{-\mathrm{j}(K_r r_i+K_s s_i-\phi_i)}\right\|_2^2 + \lambda\left\|\Delta^2 r_i\right\|_2^2\right) \tag{3}$$

Eq. (3) contains two purposes: the spatial spectrum of the solution is as close to the measured value as possible, and the curve meets the prior knowledge as much as possible, *i.e.* the curve is as smooth as possible. Details about the algorithm are referred to Ref. [47]. By introducing the continuous terrain spatial correlation constraint into the array InSAR observation model, combined with the optimization method, 3D resolution performance can be greatly improved. Compared with the traditional method, the array InSAR model can realize 50 times super-resolution in theory and about ten to twenty times in engineering. With the proposed method, a 2 m antenna can be used to obtain the same resolution of a big antenna with a length of around 20–40 m. The comparison between the three-dimensional imaging results obtained using the traditional spectral estimation method and array super-resolution imaging algorithm is shown in Fig. 11. In the comparison between Fig. 11(b) and Fig. 11(c), the elevation resolution of the traditional imaging method is limited due to the limited array antenna size. The array InSAR super-resolution algorithm effectively solves this problem and improves the 3D imaging quality.

To solve the problem of interference between multi-channel signals, a MIMO array radar orthogonal signal coding method[49–52] was proposed. Based on the 2D time-frequency coding, the spatial dimension formed by the movement of the array antenna is used to increase the dimensionality of the spatial phase coding. The multidimensional filtering model is used to realize the demodulation and separation of multiple aliasing echoes in the 3D space-time-frequency space (Fig. 12). As a result, the aliasing suppression ratio is reduced from –10 dB to –38 dB and the image quality is significantly improved (Fig. 13). To address the elastic deformation of the distributed array antenna with an aircraft tremor, the multi-baseline measurement method based on a combination of rigid and flexible baselines[53] is proposed, as shown in the diagram in Fig. 14. First, an inertial measurement system is used to measure the

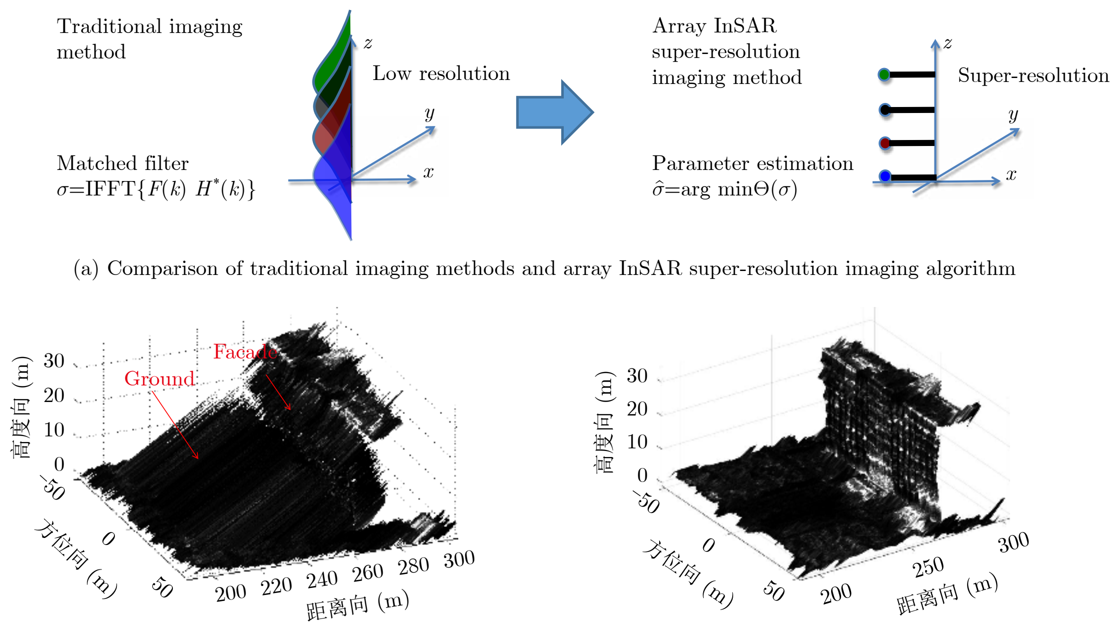

(a) Comparison of traditional imaging methods and array InSAR super-resolution imaging algorithm

(b) 3D imaging results by spectral estimation

(c) 3D imaging results by super-resolution algorithm

Fig. 11 Comparison of principles and performances of traditional methods and the array InSAR imaging method

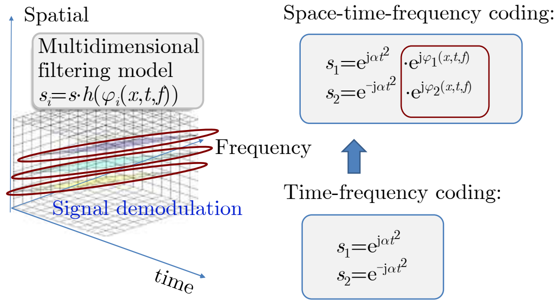

Fig. 12 Diagram of the multidimensional waveform coding

rigid part of the baseline with a precision of 1 cm. Based on this, the initial value of the three-dimensional terrain is reversed. The ground control point is used to calculate the deviation from the actual elevation. Then, the built-in error of the inertial measurement system is accurately calculated. Furthermore, the multiple baseline interference model is used to accurately invert the flexible deformation of each array node. Finally, the antenna deformation measurement and compensation with an accuracy better than 1 mm can be achieved.

In 2015, the IECAS successfully developed the first array InSAR 3D imaging system, as shown in Fig. 15. This airborne radar system adopts the side-looking imaging mode. It consists of a total of 10 array elements, with two transmitters and eight receivers forming 16 channels in the cross-track direction. The equivalent phase centers are evenly distributed. The system adopts the

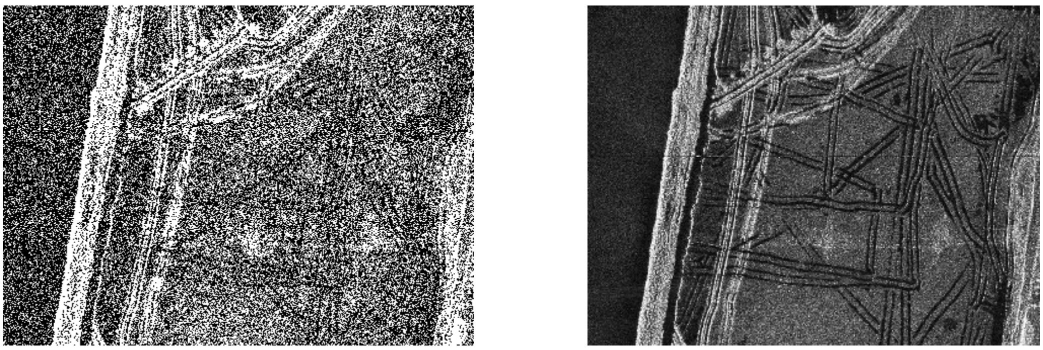

(a) Imaging result soft raditional waveform coding (b) Imaging results of multidimensional orthogonal waveform

Fig. 13 Comparison between traditional and multidimensional orthogonal waveform imaging results

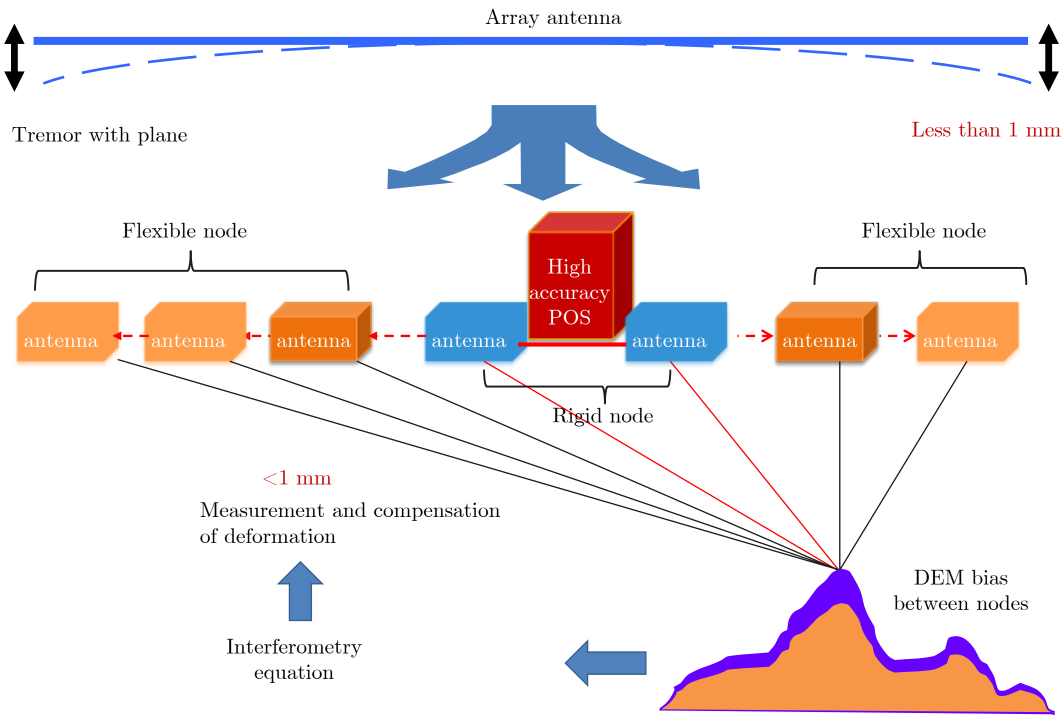

Fig. 14 Sketch of the flexible baseline measurement and compensation algorithm

frequency-modulated continuous wave and works in the Ku-band with a bandwidth of 500 MHz. The mapping swath is around 34 kms. Also in 2015, a large number of flight experiments were conducted in Shanxi. For the first time, 3D imaging of large-scale complex cities was achieved using airborne arrays. Fig. 16 shows the 3D reconstruction results of the array InSAR for a single building. As shown in Fig. 16, the layover in the original SAR image is serious, and the three parts of the ground, *i.e.*, the roof, façade and ground, are difficult to distinguish. Using the array InSAR 3D imaging method, the layover areas were distinguished. SAR 3D imaging results were obtained based on the constrained model of the buildings. The scattering information of the ground in front of the building, the texture information of the front steps, the concrete pavement, the side of the building, the structure of windows, glass curtain walls, the rain cover, and the dihedral reflection of the building are clearly shown. Fig. 17 illustrates the SAR image of the entire scene and the 3D imaging results of the array InSAR. The 3D structure of the community is clear, which confirms the high-precision urban 3D imaging capability of the array InSAR system.

(a) Airplane of array InSAR (b) Linear array (c) Processing center

Fig. 15 Array InSAR 3D imaging system by IECAS

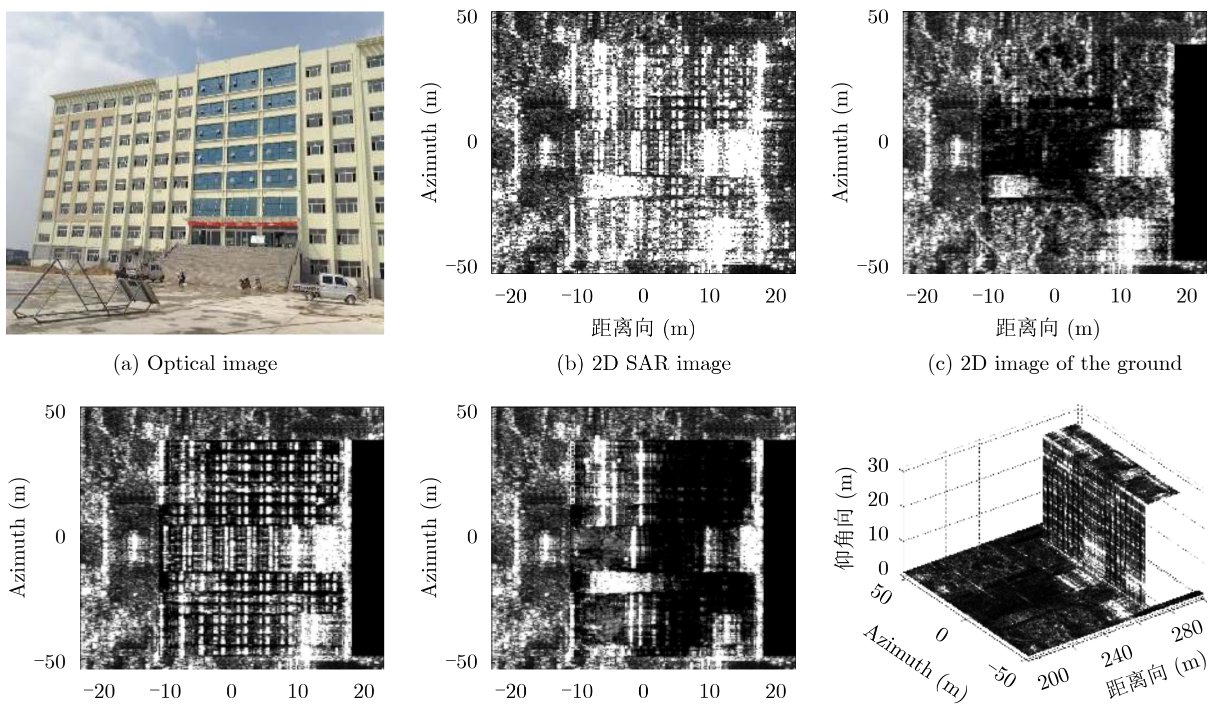

(a) Optical image (b) 2D SAR image (c) 2D image of the ground

(d) 2D image of the facade (e) 2D SAR image of the roof (f) 3D imaging results

Fig. 16 array InSAR 3D imaging results of a single building

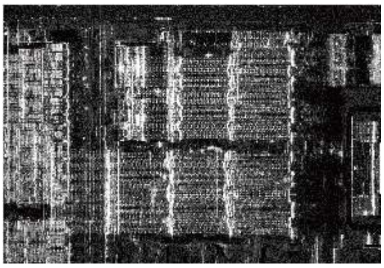

(a) SAR image of array InSAR system

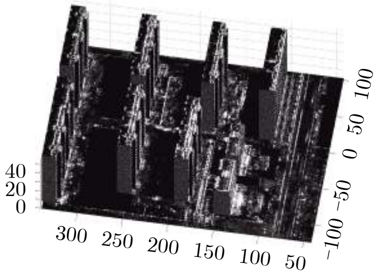

(b) 3D imaging results by array InSAR

Fig. 17 3D imaging results by the array InSAR

4 SAR Microwave Vision 3D Imaging

Based on the above analysis, the current three-dimensional imaging technology, such as TomoSAR and array InSAR, requires more than ten flights or antennas due to the need to construct an equivalent array in the elevation direction. This requirement makes it difficult to realize on a satellite, to distribute and apply, and to miniaturize. Therefore, a method to reduce the number of antennas or repeated orbit observations required for TomoSAR and array InSAR 3D imaging is at the core of the investigation in the field of SAR 3D imaging.

To solve these problems, new sources of information are needed. In fact, SAR 2D images contain 3D information, which can be perceived by trained SAR image readers, especially for 3D targets with rich information such as buildings and bridges. In addition, the scattering mechanism in the SAR echo signal also contains 3D information. It is possible to extract the structure of the scattering center through extraction of the scattering mechanism and parameter inversion. Therefore, this paper fully investigates the SAR 2D image and echo signal as a new information source, which combines the SAR imaging mechanism to realize 3D imaging. At the same time, the number of array antennas and times of repeated orbit observation are reduced. Overall, this is the basic idea of the SAR microwave vision 3D imaging method.

4.1 Concept of the SAR Microwave vision 3D imaging

SAR microwave vision 3D imaging refers to the extraction of 3D information from radar echoes and 2D images through the microwave scattering mechanism and image visual semantics mining methods. These clues are then embedded with the traditional SAR 3D imaging methods to reduce the number of multi-angle observations and realize high-efficient 3D imaging. SAR microwave vision 3D imaging is a new SAR 3D imaging method that combines the theories of computational electromagnetics, computer vision and radar signal processing.

Compared with traditional 3D imaging methods, SAR microwave vision 3D imaging has the following characteristics. First, the SAR microwave vision 3D imaging method starts from the echo, establishes the 3D scattering mapping relationship between the 3D structure of the target component and echo, and constructs the structured model of the 3D scattering mechanism of the target to increase the information for the 3D target reconstruction. Second, existing SAR 3D imaging methods proceed pixel-by-pixel in isolation, while the SAR microwave vision 3D imaging combines computer vision methods to extract semantic information from images to add constraints to the inverse problem and reduce the number of observations required.

The SAR microwave vision 3D imaging technology is different from the traditional imaging technology in terms of the information source and resolution mechanism, as shown in Tab. 1. Take the traditional SAR 2D imaging as an example. For the range direction, the resolution mechanism is the time resolution, the information source is the frequency expansion, and the processing method is pulse compression. For the azimuth direction, the resolution mechanism is angular resolution, the information source is spatial expansion, and the processing method is synthetic aperture. For the elevation resolution of the existing techniques, the resolution mechanism is also angular resolution, the source of information is spatial expansion, and the processing method is still fundamentally synthetic aperture. In the framework of the SAR microwave vision 3D imaging, the scattering mechanism and visual semantics are introduced as the information source. The processing method is a new method of SAR microwave vision 3D imaging. It can be seen that this technology is substantially different from the existing technology and is a completely new 3D imaging method.

4.2 Core scientific issues of the SAR microwave vision 3D imaging

In order to achieve the purpose of SAR microwave vision 3D imaging, it is necessary to investigate the 3D information contained in SAR echoes and 2D images. For this purpose, there is some research foundation, including methods for extracting 3D information of targets based on SAR image contents[54–56] and a 3D information inversion method based on SAR signal scattering mechanism extraction[57–59]. However, the above methods still have large limitations, and it is difficult to meet the needs of SAR microwave vision 3D imaging of complex scenes. In summary, SAR microwave vision 3D imaging requires theoretical and methodological exploratory research, mainly including three core scientific issues, the 3D microwave scattering mechanism and its inverse problem, the theory and method of three-dimensional SAR image visual cognition, and the theory and method of SAR 3D imaging based on microwave vision.

(1) 3D microwave scattering mechanism and its inverse problem

This problem is to solve how to identify the microwave scattering mechanism from the SAR echo data, and to a certain extent, reconstruct the targets' 3D cognitive parameters. Inversion of the target structure according to the scattering mechanism is an electromagnetic scattering inverse problem. Fig. 18 Due to the complex electromagnetic scattering mechanism of the actual target, the scattering characteristics of the target and its imaging characteristics in the SAR image are related to its geometrical physical parameters, such as shape and material, waveform parameters, such as frequency and polarization, observation conditions, such as angle and mode, and many other factors. Therefore, the inverse of the electromagnetic scattering must solve problems such as multiple solutions, convergence, and robustness. The 3D scattering mechanism is an important source of information for microwave vision and its identification is one of the core scientific problems to realize SAR microwave vision 3D imaging. The detection and identification of the scattering mechanism and the inversion and estimation of the 3D cognitive parameters of the target need to be solved[60,61].

Tab. 1 Comparison between SAR microwave vision 3D and traditional 3D imaging techniques

	Dimension	Resolution mechanism	Processing method	Source of information	Radar system
1st	Range	Time resolution	Range compression	Frequency expansion	Traditional radar
2nd	Azimuth	Angular resolution	Synthetic aperture	Space expansion	SAR
3rd	Elevation	Angular resolution	Synthetic aperture	Space expansion	TomoSAR and array InSAR
		Scattering mechanism visual semantics angular resolution	SAR microwave vision 3D imaging	Scattering mechanism Visual information space expansion	Microwave vision 3D SAR

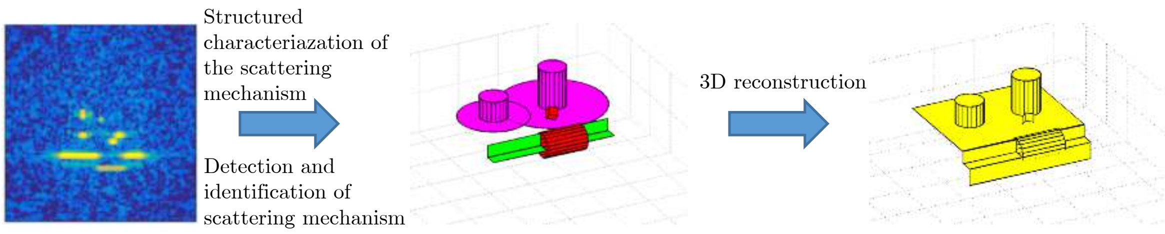

Fig. 18 Sketch of the inverse problem of electromagnetic scattering

(2) Theory and method of three-dimensional SAR image visual cognition

The theory and method of three-dimensional SAR image visual cognition is used to solve the problem of how to understand the visual semantics in SAR images, extract the 3D structure of typical targets, and to excavate 3D clues.

For optical images, the research on computer vision-based image understanding and 3D reconstruction of targets has been relatively mature. Existing studies performed a 3D reconstruction through a single optical image[62]. However, there are significant differences between SAR and optical imaging. Firstly, the imaging geometry of SAR is different from that of the optics, which is the angle projection with occlusion and no overlap, providing angle information and no depth information, while SAR is the range projection with occlusion and overlap, providing depth information but no angle information. Secondly, SAR is different from optics in the electromagnetic scattering mechanism. The optical imaging is incoherent. These images conform to the human vision habit and are smooth and insensitive to the observation angle. Generally, it is easy to acquire a large number of learning samples. As a contrast, SAR is a kind of coherent imaging and suffers from severe speckle noise and a sharp change with respect to the angle of observation. Additionally, it is difficult to acquire a large number of learning samples. These factors leads to problems such as weak robustness and poor generalization ability when the existing optical image interpretation methods are applied to the visual semantic understanding of SAR images. Therefore, current computer vision methods mainly aimed at optical images cannot be directly applied to SAR image visual understanding. It is therefore necessary to innovatively develop 3D feature mining, target representation and recognition theory of SAR image, and establish the cognitive foundation of SAR microwave 3D imaging.

(3) Theory and method of the SAR 3D imaging based on microwave vision

The theory and method of SAR 3D imaging based on microwave vision is to solve the problem of how to efficiently and accurately perform 3D imaging based on the 3D information mentioned in the previous section, which is, how to combine the microwave scattering mechanism and visual semantics with traditional SAR signal processing methods and achieve 3D imaging of complex environments.

Based on the microwave vision[63], the 3D information obtained is heterogeneous, fuzzy, and qualitative. The method to combine the hetero-

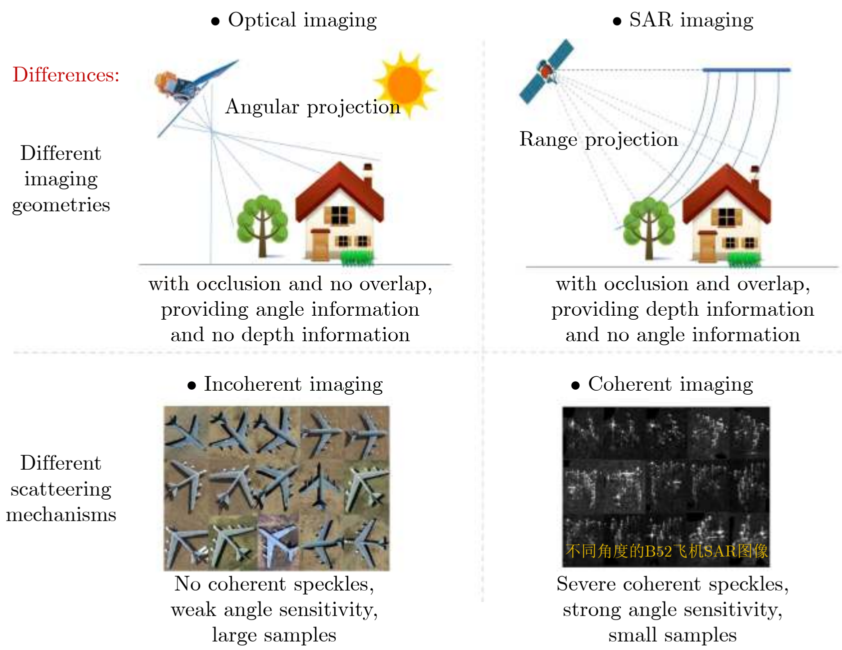

Fig. 19 Differences between the SAR and optical images

geneous and qualitative 3D clues with the quantitative SAR imaging method to achieve accurate and quantitative 3D imaging is a theoretical problem that must be solved. The existing SAR 3D imaging technology needs a lot of multi-angle observations, primarily because the solution space of the elevation parameters in the SAR image equation is too large, and the only exact solution of parameters cannot be obtained by only a few observations. If some constraints, such as the microwave scattering mechanism and image visual semantic information, are added, the solution space can be effectively reduced, and parameters of the elevation direction can be precisely determined to realize 3D imaging[64]. Therefore, it is necessary to innovatively construct a theoretical framework for SAR microwave vision 3D imaging to solve the constraints model construction of image semantics and microwave scattering mechanism and optimize heterogeneous nonlinear SAR 3D imaging equations.

The preliminary ideas are as follows. According to the SAR imaging equation,

$$\begin{cases} S_j(R_j,\eta_j) = \exp\left\{-\mathrm{j}\dfrac{4\pi R_j}{\lambda}\right\} \\ \quad \cdot \displaystyle\sum_{i=1,2,\cdots,N} |\sigma_i(h_i|R_j,\eta_j)| \exp\{\mathrm{j}\phi_i\} \\ \sqrt{\left(\sqrt{{R_j}^2 - {h_i}^2} - X_j\right)^2 + (h_i - H_j)^2} = R_j, \\ \quad i = 1,2,\cdots,N \end{cases} \tag{4}$$

The equations above are the expression of SAR single look complex images, in which R_j is the slant range, η_j is the azimuth time, λ is the wavelength, σ_i is the scattering coefficient corresponding to the ith scatterer, ϕ_i is the phase and h_i is its elevation. N is the number of scatterers overlaid on equidistant arcs, as shown in Fig. 21.

In the existing sparse 3D imaging algorithms, there are sparseness assumptions aboutσ_i, but no constraints about σ_i and h_i, which will make the solution space very large. The equations cannot be solved with a small number of observations, so the number of required multi-angle observations is large. In this technique, the constraints of visual semantics and the scattering mechanism are considered. These information will effectively reduce the solution space. The expressions are as follows.

$$\begin{cases} h_i \in f(h,x) \\ N \in \{K\}, (|\sigma_i|,\phi_i) \in \{|\sigma_K|,\phi_K\} \end{cases} \tag{5}$$

In which $h_i \in f(h,x)$ indicates that the scatterers are assumed to be on a certain curve based on the microwave vision clues. $N \in \{K\}$ means that the number of layovers is known,$(|\sigma_i|,\phi_i) \in \{|\sigma_K|,\phi_K\}$ means that there is prior information about the scattering coefficients. The 3D information can be extracted by solving these equations.

However, sometimes the explicit expression above cannot be obtained using the microwave vision method. Under these circumstances, the constraint models can be established using 3D information extracted by the scattering mechanism and visual semantics, such as the continuity constraints between pixels and the prior distribution of the parameters. Multi-constraint CS and a deep neural network are used to solve the complex multi-constraint inverse problem.

5 Conclusion

SAR 3D imaging technology can directly ob-

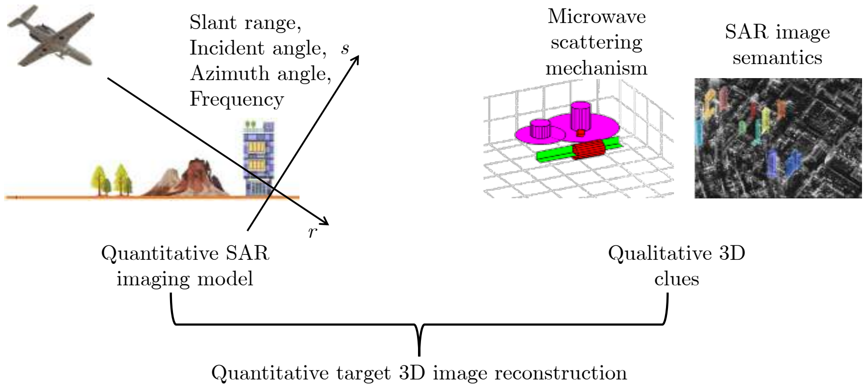

Fig. 20 SAR microwave vision 3D imaging

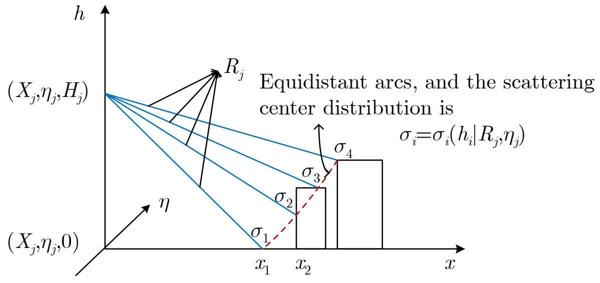

Fig. 21 Signal model of the overlapping pixel

tain the 3D electromagnetic scattering structure of a target, and plays an important role in urban mapping and disaster assessment. This paper reviews the development of the SAR 3D imaging technology and introduces in detail the characteristics of TomoSAR and array InSAR. These existing 3D imaging methods are restricted by their high complexity or long imaging period, which has limited their popularization and large-scale application.

In view of the above problems, this paper proposes the SAR microwave vision 3D imaging method. Under this framework, computational electromagnetics, computer vision and relevant theoretical methods are used to extract the 3D information in the microwave scattering mechanism and image visual semantics that are not used in existing 3D imaging methods. The 3D information is extracted and expressed as constraints on the traditional SAR signal processing to realize feeding of 3D information, which will greatly reduce the dependence on the number of spatially expanded observations. SAR 3D imaging can be achieved with a smaller number of observations, and the new method introduces a new direction for the development of SAR 3D imaging. The research of the SAR microwave vision 3D imaging is still in the early stage, and further research is needed to promote the development of SAR 3D imaging.

References

[1] GRAHAM L C. Synthetic interferometer radar for topographic mapping[J]. *Proceedings of the IEEE*, 1974, 62(6): 763–768. doi: 10.1109/PROC.1974.9516.

[2] LAPRADE G L. An analytical and experimental study of stereo for radar[J]. *Photogrammetric Engineering*, 1963, 29(2): 294–300.

[3] LEBERL F W, RAGGAM J, and KOBRICK M. On Stereo Viewing of SAR Images[J]. *IEEE Transactions on Geoscience and Remote Sensing*, 1985, GE-23(2): 110–117. doi: 10.1109/TGRS.1985.289407.

[4] KNAELL K. Three-dimensional SAR from curvilinear apertures[C]. Proceedings of the 1996 IEEE national Radar Conference, Ann Arbor, MI, USA, 1996.

[5] SCHMITT M and ZHU Xiaoxiang. Demonstration of single-pass millimeterwave SAR tomography for forest volumes[J]. *IEEE Geoscience and Remote Sensing Letters*, 2016, 13(2): 202–206. doi: 10.1109/LGRS.2015.2506150.

[6] ZHU Xiaoxiang and BAMLER R. Tomographic SAR inversion by L_1-norm regularization—the compressive sensing approach[J]. *IEEE Transactions on Geoscience and Remote Sensing*, 2010, 48(10): 3839–3846. doi: 10.1109/TGRS.2010.2048117.

[7] ZHU Xiaoxiang and BAMLER R. Very high resolution spaceborne SAR tomography in urban environment[J]. *IEEE Transactions on Geoscience and Remote Sensing*, 2010, 48(12): 4296–4308. doi: 10.1109/TGRS.2010.2050487.

[8] PASQUALI P, PRATI C, ROCCA F, *et al.* A 3-D sar experiment with EMSL data[C]. Proceedings of International Geoscience and Remote Sensing Symposium, IGARSS'95, Quantitative Remote Sensing for Science and Applications, Firenze, Italy, 1995: 784–786.

[9] REIGBER A and MOREIRA A. First demonstration of airborne SAR tomography using multibaseline L-band data[J]. *IEEE Transactions on Geoscience and Remote Sensing*, 2000, 38(5): 2142–2152. doi: 10.1109/36.868873.

[10] FORNARO G, LOMBARDINI F, and SERAFINO F. Three-dimensional multipass SAR focusing: Experiments with long-term spaceborne data[J]. *IEEE Transactions on Geoscience and Remote Sensing*, 2005, 43(4): 702–714. doi: 10.1109/TGRS.2005.843567.

[11] FORNARO G, LOMBARDINI F, PAUCIULLO A, *et al.* Tomographic processing of interferometric SAR data: Developments, applications, and future research perspectives[J]. *IEEE Signal Processing Magazine*, 2014, 31(4): 41–50. doi: 10.1109/MSP.2014.2312073.

[12] REALE D, FORNARO G, PAUCIULLO A, *et al.* Tomographic imaging and monitoring of buildings with very high resolution SAR data[J]. *IEEE Geoscience and Remote Sensing Letters*, 2011, 8(4): 661–665. doi: 10.1109/LGRS.2010.2098845.

[13] ZHU Xiaoxiang and BAMLER R. Demonstration of super-resolution for tomographic SAR imaging in urban environment[J]. *IEEE Transactions on Geoscience and Remote Sensing*, 2012, 50(8): 3150–3157.

[14] ZHU Xiaoxiang, MONTAZERI S, GISINGER C, *et al.*

Geodetic SAR tomography[J]. *IEEE Transactions on Geoscience and Remote Sensing*, 2016, 54(1): 18–35. doi: 10.1109/TGRS.2015.2448686.

[15] WANG Yuanyuan, ZHU Xiaoxiang, and BAMLER R. An efficient tomographic inversion approach for urban mapping using meter resolution SAR image stacks[J]. *IEEE Geoscience and Remote Sensing Letters*, 2014, 11(7): 1250–1254. doi: 10.1109/LGRS.2013.2290833.

[16] ZHU Xiaoxiang and BAMLER R. Super-resolution power and robustness of compressive sensing for spectral estimation with application to spaceborne tomographic SAR[J]. *IEEE Transactions on Geoscience and Remote Sensing*, 2011, 50(1): 247–258.

[17] ZHU Xiaoxiang and BAMLER R. Superresolving SAR tomography for multidimensional imaging of urban areas: Compressive sensing-based TomoSAR inversion[J]. *IEEE Signal Processing Magazine*, 2014, 31(4): 51–58. doi: 10.1109/MSP.2014.2312098.

[18] ZHU Xiaoxiang, GE Nan, and SHAHZAD M. Joint sparsity in SAR tomography for urban mapping[J]. *IEEE Journal of Selected Topics in Signal Processing*, 2015, 9(8): 1498–1509. doi: 10.1109/JSTSP.2015.2469646.

[19] TEBALDINI S and ROCCA F. Multibaseline polarimetric SAR tomography of a boreal forest at P-and L-bands[J]. *IEEE Transactions on Geoscience and Remote Sensing*, 2012, 50(1): 232–246.

[20] PONCE O, PRATS-IRAOLA P, SCHEIBER R, *et al*. First airborne demonstration of holographic SAR tomography with fully Polarimetric multicircular acquisitions at L-Band[J]. *IEEE Transactions on Geoscience and Remote Sensing*, 2016, 54(10): 6170–6196. doi: 10.1109/TGRS.2016.2582959.

[21] BI Hui, ZHANG Bingchen, and HONG Wen. *Lq* regularization-based unobserved baselines' data estimation method for tomographic synthetic aperture radar inversion[J]. *Journal of Applied Remote Sensing*, 2016, 10(3): 035014. doi: 10.1117/1.JRS.10.035014.

[22] BI Hui, LIU Jianguo, ZHANG Bingchen, *et al*. Baseline distribution optimization and missing data completion in wavelet-based CS-TomoSAR[J]. *Science China Information Sciences*, 2018, 61(4): 042302. doi: 10.1007/s11432-016-9068-y.

[23] WEI Lianhuan, BALZ T, and LIAO Mingsheng. Tomographic analysis of high-rise buildings using TerraSAR-X spotlight data with compressive sensing approach[C]. Proceedings of 2014 IEEE Geoscience and Remote Sensing Symposium, Quebec City, QC, Canada, 2014.

[24] WANG Jinfeng and PI Yiming. SAR tomography imaging via higher-order spectrum analysis[J]. *Journal of Systems Engineering and Electronics*, 2009, 20(4): 748–754.

[25] DONOHO D L. Compressed sensing[J]. *IEEE Transactions on Information Theory*, 2006, 52(4): 1289–1306. doi: 10.1109/TIT.2006.871582.

[26] BARANIUK R G. Compressive sensing[J]. *IEEE Signal Processing Magazine*, 2007, 24(4): 181–121.

[27] BARANIUK R and STEEGHS P. Compressive radar imaging[C]. Proceedings of 2007 IEEE Radar Conference, Boston, USA, 2007: 128–133.

[28] BUDILLON A, EVANGELISTA A, and SCHIRINZI G. SAR tomography from sparse samples[C]. Proceedings of 2009 IEEE International Geoscience and Remote Sensing Symposium, Cape Town, South Africa, 2009: IV-865–IV-868.

[29] BUDILLON A, EVANGELISTA A, and SCHIRINZI G. Three-dimensional SAR focusing from multipass signals using compressive sampling[J]. *IEEE Transactions on Geoscience and Remote Sensing*, 2011, 49(1): 488–499. doi: 10.1109/TGRS.2010.2054099.

[30] REN X Z and SUN F. Tomography SAR imaging strategy based on block-sparse model[J]. *Progress in Electromagnetics Research M*, 2016, 47: 191–200. doi: 10.2528/PIERM16010904.

[31] WEI Lianhuan, BALZ T, ZHANG Lu, *et al*. A novel fast approach for SAR tomography: Two-step iterative shrinkage/thresholding[J]. *IEEE Geoscience and Remote Sensing Letters*, 2015, 12(6): 1377–1381. doi: 10.1109/LGRS.2015.2402124.

[32] SHI Yilei, ZHU Xiaoxiang, and BAMLER R. Nonlocal compressive sensing-based SAR tomography[J]. *IEEE Transactions on Geoscience and Remote Sensing*, 2019, 57(5): 3015–3024. doi: 10.1109/TGRS.2018.2879382.

[33] YOON Y T, EINEDER M, YAGUE-MARTINEZ N, *et al*. TerraSAR-X precise trajectory estimation and quality assessment[J]. *IEEE Transactions on Geoscience and Remote Sensing*, 2009, 47(6): 1859–1868. doi: 10.1109/TGRS.2008.2006983.

[34] DE FLORIO S and D'AMICO S. Optimal autonomous orbit control of a remote sensing spacecraft[M]. AAIA. Spaceflight Mechanics 2009. Univelt, San Diego: AAIA, 2009: 949–968.

[35] PITZ W and MILLER D. The TerraSAR-X satellite[J]. *IEEE Transactions on Geoscience and Remote Sensing*, 2010, 48(2): 615–622. doi: 10.1109/TGRS.2009.2037432.

[36] WERMUTH M, HAUSCHILD A, MONTENBRUCK O, *et al*. TerraSAR-X rapid and precise orbit determination[C]. Proceedings of the 21st International Symposium on Space Flight Dynamics, Toulouse, Frankreich, 2009.

[37] CALTAGIRONE F. Status, results and perspectives of the Italian Earth Observation SAR COSMO-SkyMed[C]. Proceedings of European Radar Conference, Rome, Italy, 2009: 330–334.

[38] GIERULL C H. On a concept for an airborne downward-looking imaging radar[J]. *International Journal of Electronics and Communications*, 1999, 53(6): 295–304.

[39] GIRET R, JEULAND H, and ENERT P. A study of a 3D-SAR concept for a millimeter wave imaging radar onboard

an UAV[C]. Proceedings of the First European Radar Conference, The Netherlands, 2004: 201–204.

[40] NOUVEL J, JEULAND H, BONIN G, *et al*. A Ka band imaging radar: DRIVE on board ONERA motorglider[C]. Proceedings of IEEE International Symposium on Geoscience and Remote Sensing, Denver, USA, 2006: 134–136.

[41] NOUVEL J F. ONERA DRIVE project[C]. Proceedings of International Radar Conference "Surveillance for a Safer World", Bordeaux, France, 2009: 1–4.

[42] WEIß M, PETERS O, and ENDER J. First flight trials with ARTINO[C]. Proceedings of the 7th European Conference on Synthetic Aperture Radar, Friedrichshafen, Germany, 2008: 1–4.

[43] KLARE J, BRENNER A, and ENDER J. Impact of platform attitude disturbances on the 3D imaging quality of the UAV ARTINO[C]. Proceedings of the 7th European Conference on Synthetic Aperture Radar, Friedrichshafen, Germany, 2008.

[44] WEIß M and GILLES M. Initial ARTINO radar experiments[C]. Proceedings of the 8th European Conference on Synthetic Aperture Radar, Aachen, Germany, 2010: 1-4.

[45] PENG Xueming, WANG Yanping, HONG Wen, *et al*. Airborne downward looking sparse linear array 3-D SAR heterogeneous parallel simulation[J]. *Remote Sensing*, 2013, 5(10): 5304–5329. doi: 10.3390/rs5105304.

[46] PENG Xueming, WANG Yanping, TAN Weixian, *et al*. Airborne downward-looking MIMO 3D-SAR imaging algorithm based on cross-track thinned array[J]. *Journal of Electronics & Information Technology*, 2012, 34(4): 943–949.

[47] ZHANG Fubo, LIANG Xingdong, WU Yirong, *et al*. 3D surface reconstruction of layover areas in continuous terrain for multi-baseline SAR interferometry using a curve model[J]. *International Journal of Remote Sensing*, 2015, 36(8): 2093–2112. doi: 10.1080/01431161.2015.1030042.

[48] LI Hang, LIANG Xingdong, ZHANG Fubo, *et al*. A novel 3-D reconstruction approach based on group sparsity of array InSAR[J]. *Scientia Sinica Informationis*, 2018, 48(8): 1051–1064. doi: 10.1360/N112017-00023.

[49] WANG Jie, LIANG Xingdong, and CHEN Longyong. MIMO SAR system using digital implemented OFDM waveforms[C]. Proceedings of IEEE International Geoscience and Remote Sensing Symposium, Munich, Germany, 2012: 7428–7431.

[50] WANG Jie, CHEN Longyong, LIANG Xingdong, *et al*. Implementation of the OFDM chirp waveform on MIMO SAR systems[J]. *IEEE Transactions on Geoscience and Remote Sensing*, 2015, 53(9): 5218–5228. doi: 10.1109/TGRS.2015.2419271.

[51] WANG Jie, LIANG Xingdong, DING Chibiao, *et al*. An improved OFDM chirp waveform used for MIMO SAR system[J]. *Science China Information Sciences*, 2014, 57(6): 1–9.

[52] WANG Jie, DING Chibiao, LIANG Xingdong, *et al*. Research outline of airborne MIMO-SAR system with same time-frequency coverage[J]. *Journal of Radars*, 2018, 7(2): 220–234. doi: 10.12000/JR17046.

[53] Xiang M S, Ding C B, *et al*. Multi-baseline measurement method based on combination of rigid and flexible baselines[P]. China, CN201210512927.4, 2014-06-11.

[54] SPORTOUCHE H, TUPIN F, and DENISE L. Extraction and three-dimensional reconstruction of isolated buildings in urban scenes from high-resolution optical and SAR Spaceborne images[J]. *IEEE Transactions on Geoscience and Remote Sensing*, 2011, 49(10): 3932–3946. doi: 10.1109/TGRS.2011.2132727.

[55] XU Feng and JIN Yaqiu. Automatic reconstruction of building objects from multiaspect meter-resolution SAR images[J]. *IEEE Transactions on Geoscience and Remote Sensing*, 2007, 45(7): 2336–2353. doi: 10.1109/TGRS.2007.896614.

[56] ZHANG Yueting, DING Chibiao, QIU Xiaolan, *et al*. The characteristics of the multipath scattering and the application for geometry extraction in high-resolution SAR images[J]. *IEEE Transactions on Geoscience and Remote Sensing*, 2015, 53(8): 4687–4699. doi: 10.1109/TGRS.2015.2406793.

[57] POTTER L C and MOSES R L. Attributed scattering centers for SAR ATR[J]. *IEEE Transactions on Image Processing*, 1997, 6(1): 79–91.

[58] JACKSON J A, RIGLING B D, and MOSES R L. Canonical scattering feature models for 3D and bistatic SAR[J]. *IEEE Transactions on Aerospace and Electronic Systems*, 2010, 46(2): 525–541. doi: 10.1109/TAES.2010.5461639.

[59] JACKSON J A and MOSES R L. Synthetic aperture radar 3D feature extraction for arbitrary flight paths[J]. *IEEE Transactions on Aerospace and Electronic Systems*, 2012, 48(3): 2065–2084. doi: 10.1109/TAES.2012.6237579.

[60] LI Yongchen, XU Feng, and JIN Yaqiu. A complex target reconstruction characterized by canonical scattering objects[C]. Proceedings of IEEE International Geoscience and Remote Sensing Symposium, Beijing, China, 2016: 1278–1280.

[61] XU Feng, JIN Yaqiu, and MOREIRA A. A preliminary study on SAR advanced information retrieval and scene reconstruction[J]. *IEEE Geoscience and Remote Sensing Letters*, 2016, 13(10): 1443–1447. doi: 10.1109/LGRS.2016.2590878.

[62] LIU Xiaobai, ZHAO Yibiao, and ZHU Songchun. Single-view 3D scene reconstruction and parsing by attribute grammar[J]. *IEEE Transactions on Pattern Analysis and Machine Intelligence*, 2018, 40(3): 710–725. doi: 10.1109/TPAMI.2017.2689007.

[63] XU Feng and JIN Yaqiu. From the emergence of intelligent

science to the research of microwave vision[J]. *Science & Technology Review*, 2018, 36(10): 30–44.

[64] CHEN Jiankun, PENG Lingxiao, QIU Xiaolan, *et al.* A 3D building reconstruction method for SAR based on deep neural network[J]. *Scientia Sinica Informationis*, 2019, 49(11): 1–20. doi: 10.1360/N112018-00305.

DING Chibiao received a B.S. and Ph. D. degree in electronics engineering from Beihang University, Beijing, China, in 1997. Since 1997, he has been with the Institute of Electronics, Chinese Academy of Sciences, Beijing, where he is currently a Research Fellow. His research interests include advanced synthetic aperture radar systems, signal processing technology, and information systems.

QIU Xiaolan received a B.S. degree in electronic engineering and information science from the University of Science and Technology of China, Hefei, China, in 2004, and a Doctoral degree in signal and information processing from the Graduate University of Chinese Academy of Sciences, Beijing, in 2009. Since 2009, she has been with the Institute ofElectronics, Chinese Academy of Sciences, Beijing. Her research interests include synthetic aperture radar (SAR) imaging and geo-correction, SAR simulation, and SAR image interpretation. She currently serves as an Associate Editor for the IEEE GEOSCIENCE AND REMOTE SENSING LETTERS.

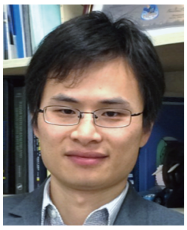

XU Feng (S'06–M'08–SM'14) received a B.E. degree (Hons.) in information engineering from Southeast University, Nanjing, China, in 2003, and a Ph.D. degree (Hons.) in electronic engineering from Fudan University, Shanghai, China, in 2008. From 2008 to 2010, he was a Postdoctoral Fellow with the NOAA Center for Satellite Application and Research (STAR), Camp Springs, MD. From 2010 to 2013, he was with Intelligent Automation Inc., Rockville, while partly working for the NASA Goddard Space Flight Center, Greenbelt, as a Research Scientist. In 2013, he joined Fudan University, where he is currently a professor with the School of Information Science and Technology.

LIANG Xingdong received a Ph.D. degree from the Beijing Institute of Technology, Beijing, China, in 2001. Since 2002, he has been with the Institute of Electronics, Chinese Academy of Science, Beijing, where he is currently a Professor of the Science and Technology on Microwave Imaging Laboratory. His research interests include real-time radar signal processing, coherent polarimetric and interferometric SAR systems.

JIAO Zekun received a B.S. degree in electronic engineering and information science from the University of Science and Technology of China, Hefei, China, in 2014, and a Doctoral degree in signal and information processing from the University of Chinese Academy of Sciences, Beijing, in 2019. Since 2019, he has been with the Institute ofElectronics, Chinese Academy of Sciences, Beijing. His research interests include synthetic aperture radar (SAR) 3D imaging.

ZHANG Fubo received a Ph.D. degree from the Institute of Electronics, Chinese Academy of Science, Beijing, China, in 2015. Since 2015, he has been with the Institute of Electronics, Chinese Academy of Science. His research interests include synthetic aperture radar tomography.